

4. DINOFLAGELLATE CYSTS FROM THE EOCENE–OLIGOCENE TRANSITION IN THE SOUTHERN OCEAN: RESULTS FROM ODP LEG 189¹

A. Sluijs,² H. Brinkhuis,² C.E. Stickley,³ J. Warnaar,²
G.L. Williams,⁴ and M. Fuller⁵

ABSTRACT

At Ocean Drilling Program (ODP) Leg 189 Sites 1170–1172, the climatologically critical Eocene–Oligocene (E–O) transition is barren of any calcareous microfossils but contains rich marine organic walled dinoflagellate cyst (dinocyst) and diatom assemblages, suitable for detailed biostratigraphic and paleoenvironmental analysis. The resulting first-ever integrated dinocyst/diatom magnetostratigraphy allows confident correlation of the E–O interval between all Leg 189 sites, including Site 1168. Our correlations indicate that the (deep) opening of the Tasmanian Gateway occurred quasi-synchronously throughout the Tasmanian region, starting at ~35.5 Ma. At Sites 1170–1172, quantitatively, three distinct dinocyst assemblages may be distinguished that reflect the relatively rapid and pronounced stepwise environmental changes associated with the E–O transition in the Tasmanian region, from a prodeltaic setting to a deep marine pelagic setting. Moreover, synchronous with the deepening of the gateway, at the southern and eastern Sites 1170–1172, typical endemic Antarctic assemblages were replaced by more cosmopolitan dinocyst communities. In marked contrast, at Site 1168 off western Tasmania, endemic Antarctic taxa are virtually absent during the E–O transition.

At Sites 1170–1172, the endemic Antarctic dinocyst assemblage (Transantarctic Flora) drastically changes into a more cosmopolitan assemblage at ~35.5 Ma, with a more offshore character, reflecting the ar-

¹Sluijs, A., Brinkhuis, H., Stickley, C.E., Warnaar, J., Williams, G.L., and Fuller, M., 2003. Dinoflagellate cysts from the Eocene–Oligocene transition in the Southern Ocean: results from ODP Leg 189. *In* Exon, N.F., Kennett, J.P., and Malone, M.J. (Eds.), *Proc. ODP, Sci. Results*, 189, 1–42 [Online]. Available from World Wide Web: <http://www-odp.tamu.edu/publications/189_SR/VOLUME/CHAPTERS/104.PDF>. [Cited YYYY-MM-DD]

²Laboratory of Palaeobotany and Palynology, Utrecht University, Budapestlaan 4, 3584CD Utrecht, The Netherlands. Correspondence author: A.Sluijs@bio.uu.nl

³Lamont-Doherty Earth Observatory, 61 Route 9W, PO Box 1000, Palisades NY 10964, USA. Present address: School of Earth, Ocean, and Planetary Sciences, Cardiff University, PO Box 914, Cardiff CF10 3YE, UK.

⁴Atlantic Geoscience Centre, PO Box 1006, Dartmouth NS B2Y 4A2 Canada.

⁵Hawaii Institute of Geophysics and Planetology, University of Hawaii at Manoa, Honolulu HI 96822, USA.

rival of different oceanographic and environmental conditions associated with the deepening of the Tasmanian Gateway. In turn, this assemblage grades at ~34 Ma into one more typical for even more off-shore and/or upwelling conditions at Site 1172. In slightly younger deposits at all sites, organic microfossils are virtually absent, reflecting winnowing and oxidation, indicative of a next step of oceanographic development. This phase may be dated as close to the Oceanic Anoxic (Oi)-1 $\delta^{18}\text{O}$ (Antarctic glaciation) event (~33.3 Ma). In a single productive sample from the earliest Oligocene the northern Site 1172, a relatively warm-water cosmopolitan assemblage has been recovered. This aspect contrasts findings from coeval deposits from the Ross Sea, where endemic Antarctic species remain dominant. Somewhere between the paleogeographic positions of Site 1172 and the Ross Sea, a strong differentiation of surface waters occurred in the earliest Oligocene, possibly reflecting the onset of the Antarctic Circumpolar Current.

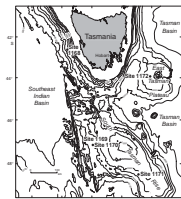
INTRODUCTION

The Cenozoic Era is remarkable in its transition from a “greenhouse” to “icehouse” Earth. Progressive high-latitude cooling eventually resulted in the formation of major ice sheets, initially on Antarctica and later in the Northern Hemisphere. This process, associated with global oceanic circulation changes, severely affected biota, resulting in closely spaced extinctions and originations of species (e.g., reviews in Berggren and Prothero, 1992). In the early 1970s, a hypothesis was proposed that climatic cooling and an Antarctic cryosphere developed as the Antarctic Circumpolar Current (ACC) progressively thermally isolated the Antarctic continent. This current is thought to have resulted from the opening of critical Antarctic conduits (i.e., the Tasmanian Gateway south of Tasmania and the Drake Passage) (Kennett, 1977; Murphy and Kennett, 1986; Shipboard Scientific Party, 2001a).

The five Ocean Drilling Program (ODP) Leg 189 sites (1168–1172; March–May 2000) (Fig. F1) were designed to test the above hypothesis and improve the understanding of Southern Ocean evolution and its relation with Antarctic and global climatic development. The relatively shallow region off Tasmania is one of the few places where well-preserved and almost-complete marine Cenozoic sequences can be drilled in paleolatitudes up to 70°S (Shipboard Scientific Party, 2001a). The basic architecture of the Paleogene sedimentary succession at Sites 1168 and 1170–1172 is similar in recording three major phases of paleoenvironmental development: (1) (Maastrichtian to) middle Eocene deposition of shallow-water siliciclastic organic-rich marine sediments during rifting between Antarctica and the South Tasman Rise, (2) a transitional condensed interval with relatively shallow water late Eocene glauconitic siliciclastic sediments giving way to earliest Oligocene deep marine pelagic carbonates representing the activation of bottom currents as the Tasmanian Gateway opened and deepened during early drifting, and (3) Oligocene–Quaternary deposition of pelagic carbonate sediments in increasingly deeper waters and more open ocean conditions as the Southern Ocean developed and expanded with the northward migration of the Australian continent (Shipboard Scientific Party, 2001a).

Shipboard palynological analysis indicated that well-preserved palynomorphs, notably organic walled dinoflagellate cysts (dinocysts) and sporomorphs are present in Maastrichtian to lowermost Oligocene strata (see Shipboard Scientific Party, 2001a; Brinkhuis, Munsterman,

F1. Leg 189 drilling locations, p. 24.



et al., and **Brinkhuis, Sengers, et al.**, both this volume). The dominance of different groups of other microfossils drastically changes with depositional environment. Calcareous groups are most prominent from the Oligocene to Quaternary, whereas siliceous groups are common from the middle Eocene to Quaternary (Shipboard Scientific Party, 2001a).

Initial onboard micropaleontological investigations indicated that the critical Eocene–Oligocene (E–O) transitional interval, related to the rapid deepening of the Tasmanian Gateway and possibly to ACC formation, is virtually devoid of calcareous microfossils at all Leg 189 sites. In contrast, the interval is marked by the occurrence of rich assemblages of palynomorphs, notably dinocysts, and rich diatom associations. Initial studies on this critical time interval indicate that the dinocyst assemblages are suitable for biostratigraphic and paleoenvironmental analyses (Shipboard Scientific Party, 2001a; **Brinkhuis, Munsterman, et al.**, and **Brinkhuis, Sengers, et al.**, both this volume).

A significant number of studies concentrating on Late Cretaceous to late Eocene dinocysts from the broad Antarctic realm or Southern Ocean are available, notably from Argentina, Southeast Australia, New Zealand, the Ross ice shelf and Seymour Island, besides several Deep Sea Drilling Program (DSDP)/ODP sites (see overviews in, e.g., Askin, 1988a, 1988b; Wilson, 1988; Wrenn and Hart, 1988; Coccozza and Clarke, 1992; Mao and Mohr, 1995; Truswell, 1997; Hannah and Raine, 1997; Hannah et al., 2000; Levy and Harwood, 2000, and Guerstein et al., 2002). These studies have documented Southern Ocean Paleogene dinocyst distribution and taxonomy in great detail. In contrast, previous studies concentrating on the E–O transition in the region are few (e.g., Clowes, 1985; Edbrooke et al., 1998). Moreover, meaningful chronostratigraphic calibration of dinocyst events in this region is largely absent. Considering that the Upper Cretaceous to Paleogene succession of, for example, Site 1172 has a robust magnetostratigraphy, intercalibrated by biotic events (**Stickley et al.**, this volume; Stickley et al., submitted [N1]), great potential to tie dinocyst events to the Geomagnetic Polarity Time Scale (GPTS) is available here.

Broad overviews of the dinocyst distribution from the Maastrichtian to the lowermost Oligocene and Quaternary intervals of Site 1172 and the upper Eocene–Quaternary of Site 1168 are presented elsewhere (**Brinkhuis, Munsterman, et al.**, and **Brinkhuis, Sengers, et al.**, both this volume). Here, we aim to present a more detailed stratigraphic analysis of the lithologically similar E–O transition at Sites 1170–1172, principally using dinocysts, and refine this correlation using relevant data that have recently become available, such as diatom events and paleomagnetic information (**Stickley et al.**, this volume, submitted [N1]). In addition, we propose correlations to Site 1168 and other Southern Ocean localities. Several new dinocyst taxa have been recorded; some of them are informally characterized herein, others are placed in broad generic groups. Future work on this material will describe these taxa formally and more details, also on other constituents of applied generic groupings, will be presented elsewhere (e.g., see Sluijs and Brinkhuis, submitted [N3]).

MATERIAL AND METHODS

During ODP Leg 189, the E–O transition was recovered at Sites 1168 (Hole 1168A), 1170 (Hole 1170D), 1171 (Holes 1171C and 1171D), and 1172 (Holes 1172A and 1172D). As indicated above, the middle Eocene

(or older) to Oligocene sedimentary succession is very similar at these sites and is basically divided into three lithostratigraphic units: (1) middle Eocene or older organic-rich brown, green, and gray relatively shallow marine silty mudstones (Site 1170: Unit V and lower Unit IV; Site 1171: Unit IV; and Site 1172: Unit III); (2) a condensed upper Eocene–lowermost Oligocene transitional unit characterized by increased glauconite content (Site 1170: upper Unit IV; Site 1171: Unit III; and Site 1172: Unit II); followed by (3) an increasingly calcareous succession of mainly nannofossil ooze that represents most of the Oligocene and the entire Neogene (Site 1170: Units III–I; Site 1171: Units II–I; and Site 1172: Unit I). Only at Site 1168 is the E–O transitional unit more expanded (see Shipboard Scientific Party, 2001b). Although these units have been recognized at all Leg 189 sites (except at Site 1169, which did not penetrate the Paleogene), they are not identically labeled because of minor local differences. For more details, see the Leg 189 *Initial Reports* volume (Exon, Kennett, Malone, et al., 2001) and further related studies (Shipboard Scientific Party, 2001a; Stickley et al., submitted [N1]). In addition, sedimentation rates clearly reflect these three distinct phases. During the middle Eocene and older interval, sedimentation rates were relatively high. From the late Eocene through the Oligocene, sedimentation rates dramatically decreased and increased locally thereafter until the present day (Stickley et al., this volume). These three basic intervals coincide with the global climate change succession of states from “Greenhouse” to “Doubthouse” to “Icehouse” as postulated in Shipboard Scientific Party (2001a). The basic units are broadly taken to represent (1) relatively shallow-marine, neritic, siliciclastic, pro-deltaic settings, which are (2) replaced by deeper-marine, current-swept settings, which eventually evolve into (3) deep marine calcareous ooze pelagic settings (Shipboard Scientific Party, 2001a). For discussion purposes we will here refer to these units as the *pro-deltaic*, *transitional*, and *pelagic* units, respectively.

In general, one sample per core section (average spacing = ~1.5 m) from Holes 1170D and 1171D were palynologically analyzed, whereas more closely spaced sampling (~10 cm) was achieved for Hole 1172A (Tables T1, T2, T3).

Palynological Processing and Analyses

Most samples were processed for semiquantitative palynological analysis. Absolute abundance data (i.e., number of palynomorphs per gram) have been generated from selected samples (indicated in Tables T1, T2, T3) via standard palynological techniques (involving spiking the samples with exote *Lycopodium*). All samples were processed at the Laboratory of Palaeobotany and Palynology, Utrecht University, The Netherlands.

Sample processing for absolute concentrations involved ~15 g of wet sediment that was dried at 60°C and weighed. After adding exote *Lycopodium*, the sample was treated with 30% hydrochloric acid (HCl) and twice with 30% hydrofluoric acid (HF) for carbonate and silicate removal, respectively. After overnight settling and neutralizing with distilled water, the supernatant was decanted. Both HF steps included 2 hr shaking and 20 hr reaction time, decanting, and addition of 30% HCl to remove fluoride gels. The residue was sieved twice using a 10-µm nylon mesh sieve to remove small particles. To break up clumps of residue, the sample was placed in an ultrasonic bath for a maximum of 5 min after the first sieving. A superficial film of residue was removed by re-

T1. Palynological results, Hole 1170D, p. 28.

T2. Palynological results, Hole 1171D, p. 30.

T3. Palynological results, Hole 1172A, p. 32.

ducing the cohesion with dissolved soap. The residue was then centrifuged (5 min; 2400 rpm), transferred to a reaction vessel with a 0.5-mL scale interval, and concentrated to 1 mL. With a micropipette, subsamples of a known volume (10–35 μL) of homogenized residue were placed on a microscope slide, embedded in glycerine jelly, and sealed with paraffin wax (cf. Boessenkool et al., 2001).

The remaining samples were processed using standard techniques. From the core samples ~15 g of wet sediment was collected and oven dried at 60°C and weighed (8–14 g). Processing involved an initial treatment in 10% HCl to dissolve carbonates, followed by a treatment of 38% HF to dissolve silicates. After each acid step, samples were washed twice by decanting after 24 hr settling and filling up with water. The HF step included 2 hr shaking at ~250 rpm and adding 30% HCl to remove fluoride gels. Then, samples were repeatedly washed in distilled water and finally sieved through a 15- μm nylon mesh sieve. To break up clumps of residue, the sample was placed in an ultrasonic bath for a maximum of 5 min after the first sieving. The residue remaining on the sieve was transferred to a glass tube. The tubes were centrifuged for 5 min at 2000 rpm and the excess amount of water was removed. For slide preparation, residues were transferred to vials and glycerine water was added. The residue was homogenized, no coloring was added, and a droplet of each residue was mounted on a slide with glycerine jelly; the mixture was stirred and sealed with nail varnish. Two slides per sample were prepared.

Slides were analyzed with a Leitz LM microscope at 400 \times or 1000 \times magnification. Where possible, slides were counted for up to 200 or more dinocysts, in addition to other associated palynomorphs. Dinocysts were counted at species level, whereas other palynomorphs were counted in broad categories (e.g., bisaccate pollen, other pollen, spores, inner linings of foraminifers [of >3 chambers in size] and acritarchs).

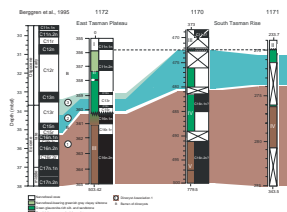
The postcruise studies are supplemented here by a few shipboard studies performed on core catcher material. Essentially, shipboard processing followed the technique described above, but a 20- μm stainless steel sieve was used (i.e., leading to the potential loss of small palynomorphs), and equipment was not as sophisticated as common modern laboratory setups. The shipboard results should therefore be taken as approximations.

Dinocyst taxonomy follows that cited in Williams et al. (1998). A species list, including remarks on previously undescribed taxa, is presented below. When *Lycopodium* numbers in a slide differed significantly from the expected calculated number (difference > 5% above or below the calculated value), the data were not included in absolute quantitative results. Images were captured using light-microscope photography (analog and digital) and scanning electron microscope (SEM). All material is stored in the collection of the Laboratory of Palaeobotany and Palynology, Botanical Palaeoecology, Utrecht University, The Netherlands.

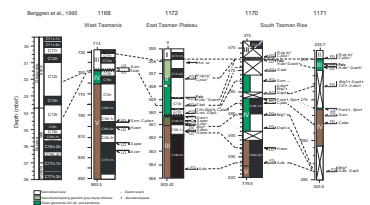
Age Models

The age models for Sites 1170–1172 as presented in [Stickley et al.](#) (this volume) are adopted here. Ages (in Ma) are indicated in Figures [F2](#) and [F3](#).

F2. Dinocysts through the Eocene–Oligocene transition, p. 25.



F3. Correlation of the Eocene–Oligocene transition among sites, p. 26.



RESULTS

General

Palynomorph and dinocyst distribution for samples from the E-O transition from Holes 1170D, 1171D, and 1172A is depicted in Tables T1, T2, and T3, respectively. Extensive discussion on the diatom events used in the regional correlation below can be found in Stickley et al. (submitted [N1]). Recovery of palynomorphs is reasonably continuous, with dinocysts being the most prominent group throughout the studied samples. Sporomorphs are common, whereas skolochorate acritarchs (of various types), remains of chlorophyte algae, and foraminiferal inner linings mainly occur at background levels.

The absolute and semiquantitative distribution patterns of the palynomorph assemblages show remarkable resemblance between the studied intervals of Sites 1170–1172 (Tables T1, T2, T3). In general, the (top of the) pro-deltaic unit is characterized by abundant marine and terrestrial palynomorphs. Dinocysts occur in high concentrations of ~15,000 dinocysts per gram sediment on average. The overlying transitional unit contains increasingly less (~4000) dinocysts and terrestrial palynomorphs per gram of sediment. The composition of the dinocyst associations differs significantly from those from the underlying siliciclastic pro-deltaic unit (Fig. F2). The boundary between the pro-deltaic unit and the overlying transitional unit is locally marked by a short palynologically barren interval (e.g., at Site 1172). At Sites 1170 and 1171 this boundary is located in nonrecovered intervals (488.3–491.5 meters below sea floor (mbsf) and 271.3–276.2 mbsf, respectively). The top part of the transitional unit at Site 1172 and the overlying oceanic unit at Sites 1170–1172 are barren of palynomorphs, except for one sample in the oceanic unit at Site 1172 (Table T3). The transition to this barren interval is sudden at all sites.

From the shipboard and first follow-up palynological studies (Shipboard Scientific Party, 2001c, 2001d, 2001e; Brinkhuis, Sengers, et al., this volume), it is apparent that the early Paleogene dinocyst stratigraphic succession at Sites 1170–1172 matches that known from other sites around the region, particularly from New Zealand (e.g., Wilson, 1988, and references therein; Crouch, 2001) and Seymour Island (Wrenn and Hart, 1988). It was also noted that during the early middle Eocene, influence of the so-called Antarctic-endemic Transantarctic dinocyst flora (cf. Wrenn and Beckmann, 1982), constituted by species like *Deflandrea antarctica*, *Octodinium askiniae*, *Enneadocysta partridgei*, *Vozzhennikovia* spp., *Spinidinium macmurdoense*, *Spinidinium luciae*, and so on, increases. The E-O transition is marked at all sites by a turnover from transantarctic dominated to associations dominated by undescribed species of *Brigantedinium?* and *Deflandrea* and *Spiniferites* spp., with slightly later the influx of *Stoveracysta kakanuiensis* at Sites 1170 and 1172. This turnover is invariably associated with the boundary between the siliciclastic pro-deltaic and transitional unit.

Qualitative and Semiquantitative Results

The younger part of the middle Eocene from Southern Ocean localities is comparatively less well studied than the older part. Only few comparisons may be made to New Zealand (e.g., Wilson, 1985, 1988; Strong et al., 1995; Edbrooke et al., 1998), DSDP Sites 280 and 281 (Crouch and Hollis, 1996), Seymour Island (Wrenn and Hart, 1988),

Scotia Sea (Mao and Mohr, 1995), and southern Argentinian successions (e.g., Guerstein et al., 2002), indicating broad similarity. The Southern Ocean middle Eocene appears to be characterized by several important last occurrences (LOs), including those of *Membranophoridium perforatum*, *Hystrichosphaeridium truswelliae*, *Arachnodinium antarcticum*, *Hystrichokolpoma spinosum*, and *Hystrichokolpoma truncatum* (Brinkhuis, Sengers, et al., this volume). The transantarctic and bipolar (restricted to polar regions on both the Northern and Southern Hemispheres) dinocysts continue to be the dominant component of the associations.

Even less is known from dinocysts from the E-O transition in the Southern Ocean. Some comparisons may be made to Southeast Australia (Browns Creek section; Cookson and Eisenack, 1965; Stover, 1975), to New Zealand (e.g., Clowes, 1985; Edbrooke et al., 1998), and to DSDP sites in the southernmost Atlantic (Goodman and Ford, 1983; Mohr, 1990). The early late Eocene dinocyst species composition at Sites 1170–1172 forms a continuation of the middle Eocene pattern. Transantarctic dinocysts predominate, and final acmes of *Enneadocysta* spp., the *D. antarctica* group, and *S. macmurdoense* are recorded.

Site 1172

So far, the E-O transition in Hole 1172A has been studied for palynology at the highest resolution of all the Leg 189 sites. Results from that hole, compared to literature, suggest that important first occurrences (FOs) across the E-O transition include those of *Schematophora speciosa*, *Aireiana verrucosa*, *Hemiplacophora semilunifera*, and *Stoveracysta ornata*. Toward the middle late Eocene the FOs of *Achomosphaera alcicornu*, *Reticulosphaera actinocoronata*, and *Alterbidinium distinctum* and the LO of *S. speciosa* are recorded, events that appear important for interregional correlation. *Vozzhennikovia* spp. continue to be a common constituent of the associations. The LO of *S. speciosa* is very close to the LO of abundant *D. antarctica* group. The latter horizon marks the boundary between the pro-deltaic and transitional unit here, signifying a marked change in the associations, including a brief barren interval. Cosmopolitan taxa like *Turbiosphaera filosa*, *Cleistosphaeridium* spp., *Spiniferites* spp., and *Lingulodinium machaerophorum* become prominent while undescribed species of *Deflandrea* and *Brigantedinium* begin to dominate the succession. Slightly higher, in a succession dated as just after the Eocene/Oligocene boundary (sensu Global Stratotype Section and Point; GSSP, Chron C13n; Stickley et al., submitted [N1]), sediments conspicuously become barren of organic microfossils to only briefly reappear in the lower Oligocene (Table T3). In this single palynomorph-bearing sample thus far from the lower Oligocene from Hole 1172A, virtually all Transantarctic Paleogene dinocysts have disappeared (only a single, poorly preserved, probably reworked specimen of *E. partridgei* was recovered). The association in this sample (189-1172A-39X-2, 3–5 cm; 356.13 mbsf) is effectively characterized by the abundance of taxa more typical for Tethyan (i.e., lower latitude) waters, including the occurrence of *Hystrichokolpoma* sp. cf. *Hystrichokolpoma oceanicum* (cf, e.g., Brinkhuis and Biffi, 1993; Wilpshaar et al., 1996; Brinkhuis, Munsterman, et al., this volume, Site 1168).

Sites 1170 and 1171

Although the E-O transition at Sites 1170 and 1171 is as yet less densely sampled, a broadly similar signature to that recovered at Site 1172 is immediately apparent (Tables T1, T2, T3). Invariably, abundant *Brigantedinium?* sp. and *Deflandrea* sp. A characterize the interval just underlying the pelagic unit. Also, *A. distinctum* is abundant. At Site 1170, *S. kakanuiensis* is locally present in these assemblages as well. Although the basal parts of the considered succession at Sites 1170 and 1171 are similar throughout to those from the siliciclastic pro-deltaic phase at Site 1172, marked differences may be noted in the transitional unit (see below, and Fig. F3).

Global Dinocyst Biostratigraphic Considerations

A comparison between the recorded late Eocene–early Oligocene dinocyst events and literature data suggest that the following dinocyst events are potentially meaningful for recognizing and globally correlating upper Eocene strata and the E/O boundary (see overviews in, e.g., Wrenn and Hart, 1988; Wilson, 1988; Brinkhuis and Biffi, 1993; Brinkhuis and Visscher, 1995; Mao and Mohr, 1995; Wilpshaar et al., 1996; Truswell, 1997; Hannah and Raine, 1997; Jaramillio and Oboh-Ikunenobe, 1999; Williams et al., this volume):

The LO of *H. semilunifera* is frequently associated with strata of late Eocene age. In Italy, this event is closely associated with the E/O boundary sensu GSSP, located just below the base of Chron C13n (e.g., Brinkhuis and Biffi, 1993). In the present study it is only recorded at Site 1172 (besides an isolated occurrence at Site 1170; see Tables T1, T3). Correlation to Hole 1172A magnetostratigraphy indicates that this event takes place in mid-Chron C16r.1r. This is markedly earlier than, for example, in Italy. This aspect may be due to the overall global cooling trend during the latest Eocene (cf., e.g., Berggren and Prothero, 1992).

Similarly, *S. speciosa* is found to occur in late Eocene deposits around the world (e.g., Brinkhuis and Biffi, 1993; Williams et al., this volume). In the present study it is only recorded at Site 1172, where it ranges from deposits assigned to Subchron C16r.1r to the top of Subchron C16n.1n (Fig. F3). In Italy, its LO is associated with the younger Chron C15 (e.g., Brinkhuis and Biffi, 1993). Again, this points to an earlier extinction at higher latitudes, possibly due to the overall global cooling trend during the latest Eocene. The event was also recorded at Site 1168 (Brinkhuis, Munsterman, et al., this volume). Current magnetostratigraphic interpretation correlates the LO of *S. speciosa* with the termination of either Subchron C17n.1n or C16n.2n at Site 1168 (Fig. F3). However, sampling resolution is as yet insufficient across the E-O transition at Site 1168. *S. speciosa* was first described from the Browns Creek section in southern Victoria, Australia (Cookson and Eisenack, 1965) and later restudied from samples from that same locality by Stover (1975). Combining their records with later generated magnetostratigraphic and calcareous microplankton data (Shafik and Idnurm, 1997), it appears that (1) this taxon does not range above the upper Eocene glauconite-rich unit at that locality and (2) it becomes extinct in deposits assigned to either Subchron C16n.2n or Chron C15n. In view of the apparent regional unconformities associated with the Subchron C16n.1n to C15n interval in the wider Tasmanian area (Shipboard Sci-

entific Party, 2001a; Stickley et al., submitted [N1]), the distribution of *S. speciosa* cannot at present be used for more precise correlation.

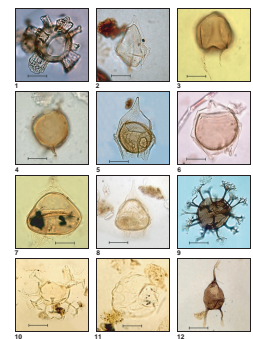
Perhaps the most significant bioevent to be associated with the globally reported mid-Chron C13n cooling (i.e., post-E/O boundary sensu GSSP) is the LO of *Areosphaeridium diktyoplokum* (see discussion in Brinkhuis and Visscher, 1995). Studies by Stover and Williams (1995) suggest that records of this taxon from the Southern Hemisphere represent a different species, namely the morphologically closely related *E. partridgei*. During our study of Leg 189 sites, in addition to *E. partridgei*, yet another morphologically closely related taxon was identified, here informally termed *Enneadocysta* sp. A. The latter may only be differentiated from *A. diktyoplokum* by being dorso-ventrally compressed (Areoligeracean style) and by having two, rather than one, antapical processes, which distally unite into a single distal perforated platform (see Pl. P1, fig. 9). This platform has the typical widened sexiform Gonyaulacean shape, a trademark of all Areoligeraceans. Locally, in Eocene assemblages from Sites 1170–1172, this taxon may dominate dinocyst associations (Shipboard Scientific Party, 2001c, 2001d, 2001e; Brinkhuis, Sengers, et al., this volume). In turn, it differs from *E. partridgei* by lacking cingular or sulcal processes and by having entire platform margins. The presence of two distally uniting antapical processes strongly suggests that the genus *Enneadocysta* should be considered to reflect a Gonyaulacoid sexiform (Areoligeracean) tabulation pattern rather than a Gonyaulacoid partiform one as suggested by Stover and Williams (1995).

Specimens of *A. diktyoplokum* sensu stricto were not recorded during the present study, despite earlier statements (Shipboard Scientific Party, 2001c) to the contrary. These specimens are herein assigned to *Enneadocysta* sp. A. Intriguingly, the recorded FOs of both *E. partridgei* and *Enneadocysta* sp. A are stratigraphically close (Brinkhuis, Sengers, et al., this volume) and closely match the timing of the FO of *A. diktyoplokum* from Northern Hemisphere records (Williams et al., this volume). The LOs of *Enneadocysta* sp. A and *E. partridgei* are less well cited than the LO of *A. diktyoplokum*, which is commonly associated with mid-Chron C13n.

Enneadocysta sp. A is not recorded above the onset of the pelagic unit, nor was it recorded at Site 1168. Its LO thus appears to be associated with the E/O boundary, like *A. diktyoplokum*. The LO of *E. partridgei* has been reported to be associated with the early/late Oligocene boundary in the Southern Ocean (e.g., Hannah and Raine, 1997). In the present study, at most localities, *E. partridgei* is a rare species in E-O transitional deposits, whereas it may dominate middle–early late Eocene assemblages (Brinkhuis, Sengers, et al., this volume). Considering (1) the abundances in the Eocene and (2) the glacial and associated ice-rafting erosive activities during the Oligocene in the Southern Ocean and (3) the clear decline in abundance over the E-O transition, early Oligocene occurrences should be regarded as reworked. In any event, the ranges of *A. diktyoplokum* and allied species seem to be very similar and lead to the speculation that they might represent different phenotypic cyst manifestations of the same dinoflagellate species, or that the species are intimately related otherwise.

The FO of *Hystrichokolpoma* sp. cf. *H. oceanicum* is reported from mid-Chron C12r from Italy (e.g., Wilpshaar et al., 1996). This matches its occurrence in coeval Site 1172 deposits (Table T3). Not only does this aspect confirm an early Oligocene age for the basal pelagic unit at Site 1172, but it also suggest warm-water influence at this time.

P1. Illustrations of taxa, p. 38.



The FO of the *S. ornata* was recorded at all studied sites in the late Eocene, including Site 1168 (Brinkhuis, Munsterman, et al., this volume), albeit with a rather scattered distribution. At Site 1172 it first occurs at the onset of Chron C15, whereas at the present low resolution studied Site 1168 its FO appears near the termination of Subchron C16n.1n or C16n.2n, depending on the magnetostratigraphic interpretation (Fig. F3). The species was described from the Browns Creek locality, Southeast Victoria, Australia, and was also reported from New Zealand (Cookson and Eisenack, 1965; Stover 1975; Clowes, 1985). Northern Hemisphere records comprise only those from the late Eocene and early Oligocene in Italy (see overview in Brinkhuis and Biffi, 1993). Available information thus indicates that it ranges from the latest middle Eocene to earliest Oligocene, with a more consistent occurrence in warmer waters.

The FO of *R. actinocoronata* was calibrated against mid-Chron C16 in central Italy (Coccioni et al., 2000). At investigated Leg 189 sites it is very rare in deposits of late Eocene age, but occurrences do suggest a Chron C16 base for this species. The same more or less holds for *Gelatia inflata*, a species first described from the late Eocene in the Bering Sea.

The other occurring species are either long ranging, not described, endemic to the Antarctic, or bipolar and therefore not useful for global correlation purposes. The above summary, although broadly confirming a late Eocene to earliest Oligocene age, does not lead to further refinements for (global) correlation. If anything, the Leg 189 records indicate earlier extinctions at this latitude than at coeval deposits at Tethyan sites.

Regional Dinocyst Biostratigraphic Considerations

A. verrucosa appears to occur in deposits calibrated against Chrons C17–C16 when combining the records of *A. verrucosa* of Cookson and Eisenack (1965) and Stover (1975) with the magneto- and biostratigraphic study of Shafik and Idnurm (1997) at Browns Creek. In the present study, *A. verrucosa* is to date only recorded in samples from Site 1172 and ranges in deposits assigned to mid-Subchron C16r.1r–mid-C16n.1n (Fig. F3). At Site 1168, depending on the magnetostratigraphic interpretation, the species occurs in deposits assigned to Subchron C16n.2n or C17n.1n (Brinkhuis, Munsterman, et al., this volume).

The FO of *S. kakanuiensis* is reported to range in the late Eocene–early Oligocene in New Zealand (Clowes 1985; G.J. Wilson, pers. comm., 2000). This event apparently also occurs in Browns Creek above the upper Eocene glauconite-rich unit there (i.e., of post-Chron C16 or C15 age, according to Shafik and Idnurm, 1997). Our results indicate the event calibrates against Chron C13r at Site 1172, and we use the event to identify that magnetochron at Sites 1170 and 1168 (Fig. F3). Future higher-resolution studies on the E–O transition at Sites 1170, 1171, and 1168 may yield more precise information. *S. kakanuiensis* potentially provides an excellent regional correlation, conspicuously appearing at the time of the deepening of the Tasmanian Gateway (e.g., Stickley et al., submitted [N1]).

The FO of *Brigantedinium?* sp. is recorded near the top of Subchron C16r.1r at Site 1172. Invariably, high abundances of this taxon mark the youngest deposits of the transitional unit. This is also recorded at Sites 1170 and 1171 and may therefore be useful for regional correlations (Fig. F2) and for paleoecological considerations discussed below. The species has not been recorded in any other E–O studies (including

Site 1168), although it is most probably conspecific with forms depicted by Mohr (1990) as “*Brigantedinium* sp.” from sediments with a similar age off Seymour Island (Site 696).

The FO of *Deflandrea* sp. A is recorded in Chron C15r at Site 1172, in the oldest palynomorph-bearing sample of the transitional unit (Table T3; Fig. F3). This event may be older at Sites 1170 and 1171, as there is a small hiatus at this level at Site 1172. This species was not recorded at Site 1168. *Deflandrea* sp. A may partly be conspecific with the as-yet only informally described species “*Deflandrea prydzensis*” (Truswell, 1997). If so, this taxon may reflect a truly high-latitude endemic signal, as records from Prydz Bay indicate an even earlier first appearance there (E.M. Truswell, M. MacPhail, pers. comm., 2002)

Quantitative Dinocyst Distribution Patterns

In terms of quantitative results, the E-O transition can be broadly characterized as a succession of three dinocyst associations, labeled 1 to 3 (Fig. F2, Tables T1, T2, T3), when data from Sites 1170–1172 are combined and correlated as proposed in Figure F3 (see below). These associations characterize the siliciclastic pro-deltaic unit (association 1), and the lower transitional unit (associations 2 and 3). The overlying upper transitional unit and the pelagic unit are virtually barren of organic matter, except for a single sample from Site 1172.

The *D. antarctica* group, *Phthanoperidinium*, *Vozzhennikovia*, and *Spinidinium* spp. dominate dinocyst association 1, whereas *E. partridgei* is common in its older parts. Dinocyst association 2 is characterized by high abundances of *Phthanoperidinium* and *Vozzhennikovia* spp., *Deflandrea* sp. A, *Brigantedinium?* sp. (and other Protoperidinaceans), *A. distinctum*, and *T. filosa*. Dinocyst association 3 (only recognized at Site 1172) is characterized by a dominance of *Brigantedinium?* sp., with locally *A. distinctum*, *Deflandrea* sp. A, *Spiniferites* spp., and *T. filosa* being common. *Cleistosphaeridium* spp., *L. machaerophorum*, and *S. kakanuiensis* may be common in this association as well.

Regional Correlation Model

Using the above qualitative and quantitative dinocyst aspects, a correlation among Sites 1170–1172 is proposed (Fig. F3). Despite the present low-resolution studies at Sites 1170 and 1171, the chronology of the events is virtually the same among Sites 1170–1172. Only the FO of *Deflandrea* sp. A appears to be older at Sites 1170 and 1171 than at Site 1172. The relatively young FO of *S. ornata* at Site 1170 is expected to be corrected in future high-resolution studies. The dinocyst events that co-occur at the boundary between the pro-deltaic and transitional units at Site 1172 are spread out over several meters at Sites 1170 and 1171. This implies a more expanded transitional unit at the latter sites, which also will be subject of future high-resolution studies.

The uppermost part of the transitional unit at Site 1172, representing earliest Oligocene strata, contains a volcanic ash layer and is palynologically barren (see also Shipboard Scientific Party, 2001e). At Sites 1170 and 1171 the volcanic ash layer was not recorded and the LO of palynomorphs co-occurs with the onset of the nannofossil ooze, implying that the top part of the transitional unit at Site 1172 was not deposited or eroded at Sites 1170 and 1171 or that oxidation and/or winnowing was/were not complete at the latter (Fig. F3). Moreover, the absence of association 3 at Sites 1170 and 1171 may be taken to indicate that the corre-

sponding strata were eroded there. Alternatively, however, association 3 may reflect local Site 1172 conditions.

At Site 1172 a relatively complete magnetostratigraphic sequence was recovered across the E-O transition (Stickley et al., this volume, submitted [N1]), providing the first-ever opportunity to calibrate Southern Ocean dinocyst records to the GPTS. For example, the new data imply that the FO of *A. distinctum* correlates with Subchron C16n.2n, the LO of abundant *D. antarctica* group with the top of Subchron C16n.1n, and the FO of *S. kakanuiensis* is calibrated against Chron C13r (see also Williams et al., this volume).

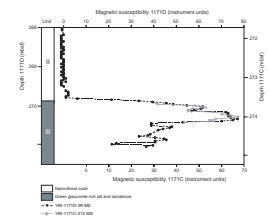
The E-O transition at Site 1170 also carries a magnetostratigraphic signal (Stickley et al., this volume). When correlating Site 1170 dinocyst events to Site 1172, it appears that normal polarity intervals originally assigned to Chrons C17n, C16n.2n, and C13n at Site 1170 (Stickley et al., this volume) are more likely to represent Subchrons C16n.2n, C16n.1n, and C11n, respectively (Fig. F3). This correlation implies that Chrons C15n and C13n are located within the core gaps at Site 1170.

To complement the dinocyst-based correlation of Leg 189 sites, new results from ongoing diatom analysis are incorporated here (as outlined in the Eocene and earliest Oligocene age model of Stickley et al., this volume). Because at Site 1171 some of the diatoms were studied in Hole 1171C and the dinocysts in Hole 1171D, an independent correlation between the two holes is needed. Core 189-1171C-31X and 189-1171D-3R are here correlated using (corrected) magnetic susceptibility (MS) (from Shipboard Scientific Party, 2001c), which in these strata mostly reflects glauconite content (Fig. F4). Core photos and MS recalibration (Fig. F4) show that the onset of the nannofossil ooze is at ~273 and ~269.9 mbsf in Holes 1171C and 1171D, respectively (not the other way around as stated in Shipboard Scientific Party, 2001c). Next, the MS curve for Hole 1171C was correlated with that for Hole 1171D taking the decrease in MS at the onset of the nannofossil ooze as a calibration point (Fig. F4). Allowing for subtle local variations, the record of Hole 1171C overlaps the Hole 1171D record almost perfectly in the uppermost part of the glauconite-rich unit. As the offset in depth appeared to be 3.6 m, diatom event depths from Hole 1171C were transferred to Hole 1171D depth by subtracting 3.6 m.

Abundant and well-preserved diatoms, several of which are age significant, were recovered in sediments of the E-O transition at Sites 1170, 1171, and 1172. At Site 1172, where the transition is more complete than at the other two sites, well-known circum-Antarctic diatom events have proved particularly useful in defining the magnetostratigraphic record for the early Oligocene (see Stickley et al., submitted [N1]). These same events are also recognized at Sites 1170 and 1171, allowing a reasonable regional correlation between all three sites. The diatom events used in this paper are the LOs of *Distephanosira architecturalis* (~33.5 Ma) and *Hemiaulus characteristicus* (~33.5 Ma) and the FOs of *Cavitatus jouseanus* (30.62 Ma) and *Rocella vigilans* (A) (30.24 Ma). *R. vigilans* (A) in this paper is the small form noted in Harwood and Maruyama (1992) as being morphologically and morphometrically distinct from the larger form therein, *R. vigilans* (B). At Sites 1170–1172, we take some of the diatom data from the age models presented in Stickley et al. (this volume). Sample resolution at these two southern sites is much poorer than that for Site 1172.

The LOs of *H. characteristicus* and *D. architecturalis* co-occur within the transitional unit at 358.8 mbsf in Hole 1172A. It appears these datums

F4. Correlation of Hole 1171C to Hole 1171D using MS, p. 27.



occur within close succession of each other in the circum-Antarctic and can be correlated to magnetochron C13n (see Stickley et al., submitted [N1], for in-depth discussion). Both of these events are truncated near the top of their ranges at ~33.5 Ma. In Hole 1170D, these two datums occur in the large depth range 454.61–478.50 mbsf, with their true stratigraphic position most likely occurring in the transitional unit (below 472 mbsf). Such a large stratigraphic interval is caused by an interval barren of all biogenic silica in Hole 1170D. This barren interval (~462.70–476.99 mbsf) contains pyritized diatoms of no age significance. In Hole 1171D, they occur together at the corrected (see above; Fig. F4) depth of 270.9 mbsf.

The FO of *C. jouseanus* is strongly suggested to be associated with Chron C12n in the circum-Antarctic, whereas that for *R. vigilans* (A) is correlated to Chron C11r (see Stickley et al., submitted [N1], for details). In Hole 1172A, both of these datums co-occur at the very base of the carbonate-bearing top ~2 m of the transitional unit at 357.39 mbsf. The range of *C. jouseanus* is probably truncated near its base (op. cit.) allowing an age of ~30.24 Ma to be assigned to this horizon. At Site 1170, these datums occur within the 454.61- to 478.50-mbsf low-recovery and barren interval. It is highly likely the true occurrence of both these datums is at ~472 mbsf at the base of the carbonate ooze. At Site 1171, both of these datums occur at the corrected (see above; Fig. F4) depth of ~269.9 mbsf.

At Site 1172, the LOs of the diatoms *H. characteristicus* and *D. architecturalis*, used to locate Chron C13n, co-occur with the onset of the palynologically barren interval. This is also the case at Site 1171 (and presumably also at Site 1170), implying synchronicity for these two events within the Tasman region within Chron C13n. Taking this (and above-mentioned arguments) into account, the upper (palynologically barren) part of the transitional unit was not deposited at Sites 1170 and 1171. This would explain why the FOs of *R. vigilans* (small) and *C. jouseanus* are recorded slightly later at the onset of the nannofossil oozes at Sites 1170 and 1171, whereas at Site 1172 they are recorded within the upper part of the transitional unit. It is therefore likely that the onset of the nannofossil ooze is synchronous among Sites 1170–1172.

Paleoecological Considerations of the Quantitative Dinocyst Distribution Patterns

Dinocyst association 1 essentially occurs throughout the middle to early late Eocene at Sites 1170–1172 (Shipboard Scientific Party, 2001c, 2001d, 2001e; Brinkhuis, Sengers, et al., this volume; Huber et al., submitted [N2]). Peridinioid cysts like *Deflandrea* and *Phthanoperidinium* spp. commonly dominate this association. Empirical evidence (summarized, e.g., in Brinkhuis et al., 1992, Brinkhuis, 1994; Firth, 1996; Stover et al., 1996) suggests that *Deflandrea* and *Phthanoperidinium* spp. represent marginal marine heterotrophic dinoflagellates closely tied to ancient deltaic settings and organic-rich facies. Other Leg 189 data (lithology, micropaleontology, and geochemistry; see Shipboard Scientific Party, 2001a, 2001c; Stickley et al, submitted [N1]) further support this aspect. Most representatives of *Deflandrea* are assigned to the *D. antarctica* group, whereas most representatives of *Phthanoperidinium* are assigned to the *P. echinatum* group. *D. antarctica* is a typical representative of the Antarctic-endemic Transantarctic Flora (cf. Wrenn and Beckmann, 1982), whereas most *Phthanoperidinium* species are common in high-latitude Eocene dinoflagellate cyst floras (Goodman and Ford,

1983; Mao and Mohr, 1995; Firth, 1996). In this association, typically *Vozzhenikovia* and *Spinidinium* (*S. macmurdoense*) spp. are abundant as well. These may be regarded to represent an overall similar signal: marginal marine, highly eutrophic, and high-latitude settings (siliciclastic pro-deltaic unit).

Of the Gonyaulacoid species (probably autotrophic) high abundances of *Enneadocysta* sp. A and *E. partridgei* typically alternate with dominances of the above peridinioids in association 1. A shipboard pilot study at Site 1170 indicated that these changes are cyclic (Shipboard Scientific Party, 2001c). It appeared that *Enneadocysta* maxima correlate to maximum nannoplankton occurrences, whereas *Deflandrea* maxima correlate to diatom maxima. This pattern prompted the suggestion that *Enneadocysta* maxima possibly reflect more offshore oligotrophic conditions, whereas *Deflandrea* maxima reflect more inshore eutrophic conditions.

Besides the Tasman region (e.g., Haskell and Wilson, 1975; Crouch and Hollis, 1996; Truswell, 1997) this Antarctic-endemic association 1 has also been found in the Eocene of McMurdo Sound (e.g., Hannah and Raine, 1997), the Ross Sea (Wrenn et al., 1998; Hannah et al., 2000), Seymour Island/Weddell Sea (e.g., Wrenn and Hart, 1988; Mohr, 1990), Bruce Bank/Scotia Sea (Mao and Mohr, 1995), Falkland Plateau (Goodman and Ford, 1983), Prydz Bay/Mac. Robertson Shelf (E.M. Truswell, pers. comm., 2002), and from Argentina and Chile (e.g., Guersten et al., 2002), and is thus widespread throughout the Antarctic region to paleolatitudes of ~60°S throughout the Eocene. Dinocysts of association 1 may hence be regarded to distinctly reflect endemic Antarctic high-latitude, marginal marine, and highly eutrophic settings. The dinoflagellate species that produce these cysts may have been adapted to high-latitude conditions while ocean circulation possibly precluded significant mixing of populations. Yet, typical cosmopolitan dinocysts like *Spiniferites* spp. and *Thalassiphora pelagica* co-occur with the endemic groups to a certain extent. Remarkably, association 1 dinocysts are virtually absent in coeval strata at Site 1168, off western Tasmania (Brinkhuis, Munsterman, et al., this volume). Instead, only largely cosmopolitan to typical lower-latitude species are abundant at Site 1168 across the E-O transition. This suggests that water masses influencing that locality were distinct from those influencing all other Leg 189 sites at this time. This aspect and possible paleoenvironmental and paleoceanographical consequences are further discussed elsewhere (Huber et al., submitted [N1]).

At ~35.5 Ma (early late Eocene), association 1 was abruptly or gradually replaced by dinocyst associations 2 and/or 3 at Sites 1170–1172. In modern oceans, representatives of *Brigantedinium* are characteristic for coastal and oceanic upwelling regions as well as sea ice conditions and possibly frontal regions (e.g., Wall et al., 1977; Rochon et al., 1999). *Brigantedinium* spp. represent heterotrophic dinoflagellates, typically feeding on diatoms. The FO and later abundance of *Brigantedinium?* sp. might indicate the installment of an (oceanic) upwelling system on a large scale. Combined Leg 189 data confirm this aspect, reflecting the deepening of the Tasmanian Gateway (see also Stickley et al., submitted [N1]). Abundant *Spiniferites* spp. implies more cosmopolitan waters. From this point of view, the endemic aspect of the associations declines during deposition of the transitional unit. *Brigantedinium?* sp. may be seen as endemic to the Antarctic, as it was never found in other E-O transitional associations worldwide, except from the Antarctic Site 696 (Mohr, 1990). This taxon is separated from *Brigantedinium* sensu stricto

in view of it having a thin outer wall, not known from modern or fossil *Brigantedinium*. If this aspect, which may be related to preservation (also not always seen on specimens analyzed here), is discarded, it is difficult to separate representatives of this taxon from modern *Brigantedinium* (see also Brinkhuis, Sengers, et al., this volume). This would make them cosmopolitan, invariably associated with high nutrient oceanic settings.

At ~35.5 Ma at Sites 1170 and 1171, not only *Brigantedinium?* sp. but also other Protoperidinioid (heterotrophic) taxa like *O. askiniae* and *Selenopemphix* spp. became abundant (Tables T1, T2). It appears that the deepening event was synchronous among Sites 1170–1172 and even affected Site 1168 off western Tasmania, and possibly even localities such as Browns Creek (Southeast Australia; considering the unconformities in these strata) (Shafik and Idnurm, 1997) (see Fig. F3). If compared to similar data from off Seymour Island (ODP Site 696) (Mohr, 1990), a similar signal and timing are apparent on the other side of Antarctica.

At ~34 Ma, dinocyst association 2 was gradually replaced by association 3. This association, so far only recorded at Site 1172, is dominated by representatives of *Brigantedinium?* sp. Slightly younger deposits, from ~33.5 Ma, are virtually devoid of organic matter. This aspect is most probably related to increased winnowing and oxidation. This transition occurs close to the timing of the Oi-1 $\delta^{18}\text{O}$ event of Zachos et al. (1992, 1994) at ~33.3 Ma. The latter event is widely seen to reflect the onset of major Antarctic ice sheet formation and concomitant cooling of surface and deep waters. Inception of cooler O_2 -rich bottom waters, as well as a stronger deepwater flow regime, may well have been responsible for the virtual disappearance of organic matter at Leg 189 sites at this time. Remarkably, however, in the single palynomorph-bearing sample thus far from the lowermost Oligocene (at ~32 Ma from Hole 1172A), virtually all Transantarctic Paleogene dinocysts have disappeared. This earliest Oligocene association is, perhaps surprisingly, characterized by the abundance of taxa more typical for Tethyan (i.e., lower latitude) waters. This assemblage markedly differs from age-equivalent ones recovered from the Ross Sea farther to the southeast (e.g., Hannah et al., 2000). There, apparently endemic protoperidinioid dinocyst communities continue to dominate the assemblages. The change in associations at Site 1172 signifies the introduction of completely different surface waters in early Oligocene times in this region. Unfortunately, no data from the coeval intervals of the Oligocene of Sites 1170 and 1171 are available at this stage, as samples are nonproductive (see Tables T1, T2). It may be speculated that somewhere between the Ross shelf and Site 1172 the ecological- or water mass-controlled boundary between these associations occurred, possibly even to the north of Sites 1170 and 1171. Further aspects and consequences of these findings are discussed in Stickley et al. (submitted) [N1] and Huber et al. (submitted) [N2].

CONCLUDING REMARKS

Our studies resulted in an unprecedented integrated biomagnetostratigraphic record across the E-O transition, providing the first ever calibration for Southern Ocean dinocyst records. It now appears that several LOs of cosmopolitan species (e.g., *H. semilunifera* and *S. speciosa*) are older here than they are in the Tethyan realm (e.g., Brinkhuis and Biffi, 1993). This aspect may be due to the overall global cooling trend during the latest Eocene, resulting in equatorward migration of cosmo-

opolitan taxa from the higher latitudes. Further integration and comparison of these and coeval circum-Antarctic endemic events (see compilation in [Williams et al.](#), this volume), widely recorded around Antarctica in previous studies, will lead to better assessment of the timing of paleoenvironmental changes in the Paleogene of the Southern Ocean, notably in shallow-marine domains.

For the first time, integrated biomagnetostratigraphy allows detailed age assessment of the critical deepening of the Tasmanian Gateway. Our correlations indicate that this event occurred quasi-synchronously throughout the Tasmanian region, starting at ~35.5 Ma, some 2 m.y. before the E/O boundary. Quantitatively, the succession of three distinct dinocyst assemblages reflects the relatively rapid and pronounced stepwise environmental changes associated with the E-O transition in the Tasmanian region.

The oldest association reflects a pro-deltaic setting that prevailed in the region since the Cretaceous (see also [Brinkhuis, Sengers, et al.](#), this volume). This association has been recognized all around the Antarctic margin and is known as the Transantarctic Flora (cf., e.g., Wrenn and Beckman, 1982). In marked contrast, at Site 1168 off western Tasmania, these endemic Antarctic taxa are conspicuously absent in upper Eocene deposits ([Brinkhuis, Munsterman, et al.](#), this volume). This aspect indicates that surface waters influencing Site 1168 were distinctly different than those at the other Leg 189 sites (see [Stickley et al.](#), submitted [N1]; [Huber et al.](#), submitted [N2]). At Sites 1170–1172, this Transantarctic Flora assemblage drastically changes into a more cosmopolitan assemblage at ~35.5 Ma, generally with a more offshore character. This reflects the arrival of different oceanographic and environmental conditions associated with the deepening of the Tasmanian Gateway. In turn, this assemblage grades at ~34 Ma into one more typical for even more offshore and/or upwelling conditions at Site 1172. In slightly younger deposits at all sites, organic microfossils are virtually absent, reflecting winnowing and oxidation, indicative of a next step of oceanographic development. This phase may be dated as very near or at the Oi-1 $\delta^{18}\text{O}$ (Antarctic glaciation) event of [Zachos et al.](#) (1992, 1994) (~33.3 Ma), and it appears that the two phenomena may be intrinsically connected. In a single productive sample from the earliest Oligocene at the northern Site 1172, a relatively warm water cosmopolitan assemblage was recovered. This aspect contrasts findings from coeval deposits from the Ross Sea, where endemic Antarctic species remain dominant ([Hannah et al.](#), 2000). Thus, somewhere between the paleo-positions of Site 1172 and the Ross Sea, a strong differentiation of surface waters occurred in the earliest Oligocene, possibly reflecting the onset of the Antarctic Circumpolar Current.

ACKNOWLEDGMENTS

This research used samples and data provided by the Ocean Drilling Program (ODP). ODP is sponsored by the U.S. National Science Foundation (NSF) and participating countries under management of Joint Oceanographic Institutions (JOI) Incorporated. Funding for this research was provided by US and international agencies. A.S., H.B., and J.W. thank NWO, the Netherlands Organization for Scientific Research. Funding for the diatom research was provided to CES by the Natural Environment Research Council (NERC)/UK-ODP to CES. CES gratefully

acknowledges the Environmental Change Research Centre (University College London, UK).

Reviewers Fabienne Marret, Jens Matthiessen, Mitch Malone, and Lorri Peters are kindly thanked for critical reading and comments. We thank Natasja Welters and Jan van Tongeren (Utrecht) for sample processing. Leonard Bik (Utrecht) is kindly thanked for electronic photography handling and general assistance. The crew of Leg 189 is thanked for general support. This is the Netherlands School of Sedimentary Geology (NSG) contribution number 2003.09.03.

REFERENCES

- Askin, R.A., 1988a. Campanian to Paleogene palynological succession of Seymour and adjacent islands, northern Antarctic Peninsula. In Feldmann, R.M., and Woodburne, M.O. (Eds.), *Geology and Paleontology of Seymour Island, Antarctic Peninsula*. Mem.—Geol. Soc. Am., 169:131–153.
- , 1988b. The palynological record across the Cretaceous/Tertiary transition on Seymour Island, Antarctica. In Feldmann, R.M., and Woodburne, M.O. (Eds.), *Geology and Paleontology of Seymour Island, Antarctic Peninsula*. Mem.—Geol. Soc. Am., 169:155–162.
- Berggren, W.A., and Prothero, D. (Eds.), 1992. *Eocene–Oligocene Climatic and Biotic Evolution*: Princeton (Princeton Univ. Press).
- Boessenkool, K.P., van Gelder, M.-J., Brinkhuis, H., and Troelstra, S.R., 2001. Distribution of organic-walled dinoflagellate cysts in surface sediments from transects across the Polar Front offshore Southeast Greenland. *J. Quat. Sci.*, 16:661–666.
- Brinkhuis, H., 1994. Late Eocene to early Oligocene dinoflagellate cysts from the Priabonian type-area (Northeast Italy): biostratigraphy and paleoenvironmental interpretation. *Palaeogeogr., Palaeoclimatol., Palaeoecol.*, 107:121–163.
- Brinkhuis, H., and Biffi, U., 1993. Dinoflagellate cyst stratigraphy of the Eocene/Oligocene transition in central Italy. *Mar. Micropaleontol.*, 22:131–183.
- Brinkhuis, H., Powell, A.J., and Zevenboom, D., 1992. High-resolution dinoflagellate cyst stratigraphy of the Oligocene/Miocene transition interval in Northwest and central Italy. In Head, M.J., and Wrenn, J.H. (Eds.), *Neogene and Quaternary Dinoflagellate Cysts and Acritarchs*: Salt Lake City (Publishers Press), 219–258.
- Brinkhuis, H., and Visscher, H., 1995. The upper boundary of the Eocene Series: a reappraisal based on dinoflagellate cyst biostratigraphy and sequence stratigraphy. In Berggren, W.A., Kent, D.V., Aubry, M.-P., and Hardenbol, J. (Eds.), *Geochronology, Time Scales and Global Stratigraphic Correlation*. Spec. Publ.—SEPM, 54:295–304.
- Clowes, C.D., 1985. *Stoveracysta*, a new gonyaulacacean dinoflagellate genus from the upper Eocene and lower Oligocene of New Zealand. *Palynology*, 9:27–35.
- Coccioni, R., Basso, D., Brinkhuis, H., Galeotti, S., Gardin, S., Monechi, S., and Spezzaferrri, S., 2000. Marine biotic signals across a late Eocene impact layer at Massignano, Italy: evidence for long-term environmental perturbations? *Terra Nova*, 12:258–263.
- Cocozza, C.D., and Clarke, C.M., 1992. Eocene microplankton from La Meseta Formation, northern Seymour Island. *Antarct. Sci.*, 4:355–362.
- Cookson, I.C., and Eisenack, A., 1965. Microplankton from the Browns Creek clays, SW Victoria. *Proc. R. Soc. Victoria*, 79:119–137.
- Crouch, E.M., 2001. Environmental change at the Paleocene–Eocene biotic turnover [Ph.D. thesis]. Utrecht University, Utrecht, The Netherlands.
- Crouch, E.M., and Hollis, C.J., 1996. Paleogene palynomorph and radiolarian biostratigraphy of DSDP Leg 29, Sites 280 and 281, South Tasman Rise. *Inst. Geol. Nucl. Sci., Sci. Rep.*, 96:1–46.
- Edbrooke, S.W., Crouch, E.M., Morgans, H.E.G., and Sykes, R., 1998. Late Eocene–Oligocene Te Kuiti Group at Mount Roskill, Auckland, New Zealand. *N. Z. J. Geol. Geophys.*, 41:85–93.
- Exon, N.F., Kennett, J.P., Malone, M.J., et al., 2001. *Proc. ODP, Init. Repts.*, 189 [CD-ROM]. Available from: Ocean Drilling Program, Texas A&M University, College Station TX 77845-9547, USA.
- Firth, J.V., 1996. Upper middle Eocene to Oligocene dinoflagellate biostratigraphy and assemblage variations in Hole 913B, Greenland Sea. In Thiede, J., Myhre, A.M., Firth, J.V., Johnson, G.L., and Ruddiman, W.F. (Eds.), *Proc. ODP, Sci. Results*, 151: College Station, TX (Ocean Drilling Program), 203–242.
- Goodman, D.K., and Ford, L.N., Jr., 1983. Preliminary dinoflagellate biostratigraphy for the middle Eocene to Lower Oligocene from the Southwest Atlantic Ocean. In

- Ludwig, W.J., Krasheninnikov, V.A., et al., *Init. Repts. DSDP*, 71: Washington (U.S. Govt. Printing Office), 859–977.
- Guerstein, G.R., Chiesa, J.O., Guler, M.V., and Camacho, H.H., 2002. Biostratigrafía basada en quistes de dinoflagelados de la Formación Cabo Pena (Eoceno terminal-Oligoceno temprano), Tierra del Fuego. *Argent. Rev. Esp. Micropal.*, 34:105–116.
- Hannah, M.J., and Raine, J.I. (Eds.), 1997. Southern Ocean Late Cretaceous/early Cenozoic biostratigraphic datums: a report of the Southern Ocean paleontology workshop. *Sci. Rep.–Inst. Geol. Nucl. Sci.*, 4:1–33.
- Hannah, M.J., Wilson, G.J., and Wrenn, J.H., 2000. Oligocene and Miocene marine palynomorphs from CRP-2/2A, Victoria Land Basin, Antarctica. *Terra Antart.*, 7:503–511.
- Harwood, D.M., and Maruyama, T., 1992. Middle Eocene to Pleistocene diatom biostratigraphy of Southern Ocean sediments from the Kerguelen Plateau, Leg 120. In Wise, S.W., Jr., Schlich, R., et al., *Proc. ODP, Sci. Results*, 120: College Station, TX (Ocean Drilling Program), 683–733.
- Haskell, T.R., and Wilson, G.L., 1975. Palynology of Sites 280–284, DSDP Leg 29, off southeastern Australia and western New Zealand. In Kennett, J.P., Houtz, R.E., et al., *Init. Repts. DSDP*, 29: Washington (U.S. Govt. Printing Office), 731–741.
- Jaramillio, C.A., and Oboh-Ikunenobe, F.E., 1999. Sequence stratigraphic interpretations from palynofacies, dinocyst and lithological data of upper Eocene–lower Oligocene strata in southern Mississippi and Alabama, U.S. Gulf Coast. *Palaeogeogr., Palaeoclimatol., Palaeoecol.*, 145:259–302.
- Kennett, J.P., 1977. Cenozoic evolution of Antarctic glaciation, the circum-Antarctic Ocean, and their impact on global paleoceanography. *J. Geophys. Res.*, 82:3843–3860.
- Levy, R.H., and Harwood, D.M., 2000. Tertiary marine palynomorphs from the McMurdo Sound erratics, Antarctica. *Antarct. Res. Ser.*, 76:183–242.
- Mao, S., and Mohr, B.A.R., 1995. Middle Eocene dinocysts from Bruce Bank (Scotia Sea, Antarctica) and their palaeoenvironmental and palaeogeographic implications. *Rev. Palaeobot. Palynol.*, 86:235–263.
- Mohr, B.A.R., 1990. Eocene and Oligocene sporomorphs and dinoflagellate cysts from Leg 113 drill sites, Weddell Sea, Antarctica. In Barker, P.F., Kennett, J.P., et al., *Proc. ODP, Sci. Results*, 113: College Station, TX (Ocean Drilling Program), 595–612.
- Murphy, M.G., and Kennett, J.P., 1986. Development of latitudinal thermal gradients during the Oligocene: oxygen-isotope evidence from the southwest Pacific. In Kennett, J.P., von der Borch, C.C., et al., *Init. Repts. DSDP*, 90: Washington (U.S. Govt. Printing Office), 1347–1360.
- Rochon, A., de Vernal, A., Turon, J.L., Mathiessen, J., and Head, M.J., 1999. Distribution of recent dinoflagellate cysts in surface sediments from the North Atlantic Ocean and adjacent seas in relation to sea-surface parameters. *Am. Assoc. Stratigr. Palynol. Contrib. Ser.*, Vol. 35.
- Shafik, S., and Idnurm, M., 1997. Calcareous microplankton and polarity reversal stratigraphies of the upper Eocene Browns Creek clay in the Otway Basin, southeast Australia: matching the evidence. *Aust. J. Earth Sci.*, 44:77–86.
- Shipboard Scientific Party, 2001a. Leg 189 summary. In Exxon, N.F., Kennett, J.P., Malone, M.J., et al., *Proc. ODP, Init. Repts.*, 189, 1–98 [CD-ROM]. Available from: Ocean Drilling Program, Texas A&M University, College Station TX 77845-9547, USA.
- , 2001b. Site 1168. In Exxon, N.F., Kennett, J.P., Malone, M.J., et al., *Proc. ODP, Init. Repts.*, 189, 1–170 [CD-ROM]. Available from: Ocean Drilling Program, Texas A&M University, College Station TX 77845-9547, USA.
- , 2001c. Site 1170. In Exxon, N.F., Kennett, J.P., Malone, M.J., et al., *Proc. ODP, Init. Repts.*, 189, 1–167 [CD-ROM]. Available from: Ocean Drilling Program, Texas A&M University, College Station TX 77845-9547, USA.
- , 2001d. Site 1171. In Exxon, N.F., Kennett, J.P., Malone, M.J., et al., *Proc. ODP, Init. Repts.*, 189, 1–176 [CD-ROM]. Available from: Ocean Drilling Program, Texas A&M University, College Station TX 77845-9547, USA.

- , 2001e. Site 1172. In Exon, N.F., Kennett, J.P., Malone, M.J., et al., *Proc. ODP, Init. Repts.*, 189, 1–149 [CD-ROM]. Available from: Ocean Drilling Program, Texas A&M University, College Station TX 77845-9547, USA.
- Stover, L.E., 1975. Observations on some Australian Eocene dinoflagellates. *Geoscience and Man. Proc. 6th Annu. Mtg. Am. Assoc. Stratigr. Palynol.*, 11:35–45.
- Stover, L.E., Brinkhuis, H., Damassa, S.P., de Verteuil, L., Helby, R.J., Monteil, E., Partridge, A.D., Powell, A.J., Riding, J. B., Smelror, M., and Williams, G.L., 1996. Mesozoic–Tertiary dinoflagellates, acritarchs and prasinophytes. In Jansonius, J., and McGregor, D.C. (Eds.), *Principles and Applications* (Vol. 2): College Station, TX (Am. Assoc. Stratigraphic Palynol. Found.), 641–750.
- Stover, L.E., and Williams, G.L., 1995. A revision of the Paleogene dinoflagellate genera *Areosphaeridium* Eaton 1971 and *Eatonicysta* Stover and Evitt 1978. *Micropaleontology*, 41:97–141.
- Strong, C.P., Hollis, C.J., and Wilson, G.J., 1995. Foraminiferal, radiolarian, and dinoflagellate biostratigraphy of Late Cretaceous to middle Eocene pelagic sediments (Muzzle Group), Mead Stream, Marlborough, New Zealand. *N. Z. J. Geol. Geophys.*, 38:171–209.
- Truswell, E.M., 1997. Palynomorph assemblages from marine Eocene sediments on the west Tasmanian continental margin and the South Tasman Rise. *Aust. J. Earth Sci.*, 44:633–654.
- Wall, D., Dale, B., Lohmann, G.P., and Smith, W.K., 1977. The environmental and climatic distribution of dinoflagellate cysts in modern marine sediments from regions in the North and South Atlantic Oceans and adjacent seas. *Mar. Micropaleontology*, 2:121–200.
- Williams, G.L., Lentin, J.K., and Fensome, R.A., 1998. *The Lentin and Williams Index of Fossil Dinoflagellate Cysts* (1998 ed.). Am. Assoc. Stratigr. Palynol., Contrib. Ser., Vol. 34.
- Wilpshaar, M., Santarelli, A., Brinkhuis, H., and Visscher, H., 1996. Dinoflagellate cysts and mid-Oligocene chronostratigraphy in the central Mediterranean region. *J. Geol. Soc. London*, 153:553–561.
- Wilson, G.J., 1985. Dinoflagellate biostratigraphy of the Eocene Hampden Section, North Otago, New Zealand. *N. Z. Geol. Surv. Rec.*, 8:93–101.
- , 1988. Paleocene and Eocene dinoflagellate cysts from Waipawa, Hawkes Bay, New Zealand. *N. Z. Geol. Surv. Bull.*, 57:1–96.
- Wrenn, J.H., and Beckmann, S.W., 1982. Maceral, total organic carbon, and palynological analyses of Ross Ice Shelf Project site J9 cores. *Science*, 216:187–189.
- Wrenn, J.H., Hannah, M.J., and Raine, J.I., 1998. Diversity and palaeoenvironmental significance of late Cainozoic marine palynomorphs from the CRP-1 core, Ross Sea, Antarctica. *Terra Antart.*, 5:553–570.
- Wrenn, J.H., and Hart, G.F., 1988. Paleogene dinoflagellate cyst biostratigraphy of Seymour Island, Antarctica. *Mem.—Geol. Soc. Am.*, 169:321–447.
- Zachos, J.C., Breza, J.R., and Wise, S.W., 1992. Early Oligocene ice-sheet expansion on Antarctica: stable isotope and sedimentological evidence from Kerguelen Plateau, southern Indian Ocean. *Geology*, 20:569–573.
- Zachos, J.C., Stott, L.D., and Lohmann, K.C., 1994. Evolution of early Cenozoic marine temperatures. *Paleoceanography*, 9:353–387.

APPENDIX

Species List and Taxonomic Remarks

Achomosphaera alvicornu

Achomosphaera ramulifera

Aireiana verrucosa

Alterbidinium distinctum

Alterbidinium spp.

Areoligera? *semicirculata*

Batiacasphaera spp.

Remarks: This group constitutes several new species, to be formally described elsewhere.

Brigantedinium? sp.

Remarks: This species is throughout comparable to species of *Brigantedinium*, but differs by having a distinct periphragm, in ideally preserved cases displaying a long, slender apical horn, besides two long and slender antapical horns. The length of the horns may be as much as four times the diameter of the central body. This outer wall is delicate and thin and is often either removed through oxidation or mechanical disturbance, or may be present as a wrinkled, poorly defined thin outer membrane. Since *Brigantedinium* species are considered acavate, the species is questionably attributed here to the genus. The species is most probably conspecific with forms depicted by Mohr (1990) as "*Brigantedinium* sp." from sediments with a similar age off Seymour Island (Site 696). The species will be formally described elsewhere.

Cerebrocysta spp.

Remarks: This group constitutes several new species, to be formally described elsewhere.

Cleistosphaeridium spp.

Cordosphaeridium minimum

Corrudinium spp.

Remarks: This group constitutes several new species, to be formally described elsewhere.

Dapsilidinium spp.

Deflandrea antarctica group

Remarks: Forms morphologically ranging between *D. antarctica* and *Deflandrea cygniformis* are combined in this group (essentially all forms with a distinct "bell-shaped" hypotract and relatively short antapical horns).

Deflandrea convexa group

Remarks: Forms of *Deflandrea* characterized by a condensed periphragm are combined in this group.

Deflandrea phosphoritica group

Remarks: Forms of *Deflandrea* characterized by having a periphragm corresponding to the general periphragmal outline of *D. phosphoritica* are combined in this group, regardless of ornamentation of the periphragm and/or endophragm (e.g., including *D. granulosa*, *D. granulata*, *D. robusta*, *D. spinosa*, *D. heterophlycta*, and *D. webbii*)

Deflandrea sp. A

Remarks: This rather large species of *Deflandrea* may be characterized by a distinctly triangular endophragm and by having a relatively long apical and short antapical horns. It is possibly partly conspecific with *Deflandrea prydzensis* of Truswell, 1997. The species will be formally described elsewhere.

Diphyes colligerum

Distatodinium spp.

Elytrocysta spp.

Enneadocysta partridgei

Enneadocysta pectiniformis

Enneadocysta sp. A

Remarks: This species of *Enneadocysta* closely resembles *Areosphaeridium diktyoplokum* but differs by having two antapical processes, distally united by a single perforated platform, and by being dorso-ventrally compressed. The latter features are more typical for *Enneadocysta*, although clearly the form (and other species of *Enneadocysta*) is/are gonyaulacoid sexiform rather than partiform as suggested by Stover and Williams (1995). The species will be formally described elsewhere.

Eocladopyxis spp.

Remarks: This group constitutes several new species, to be formally described elsewhere.

Gelatia inflata

Glaphyrocysta spp.

Remarks: This group constitutes several new species, to be formally described elsewhere.

Hemiplacophora semilunifera

Histiocysta spp.

Hystrichokolpoma rigaudiae

Hystrichokolpoma sp. cf *Homotryblium oceanicum* Wilpshaar et al., 1996

Hystrichosphaeridium truswelliae

Hystrichosphaeropsis spp.

Hystrichostrogylon spp.

Impagidinium spp.

Remarks: This group constitutes several new species, to be formally described elsewhere.

Lejeunecysta spp.

Lingulodinium machaerophorum

Melitasphaeridium pseudorecurvatum

Nematosphaeropsis spp.

Octodinium askinia

Operculodinium spp.

Palaeocystodinium spp.

Paucisphaeridium spp.

Remarks: This group constitutes several new species, to be formally described elsewhere.

Phthanoperidinium echinatum group

Phthanoperidinium spp.

Remarks: This group constitutes several new species, to be formally described elsewhere.

Pyxidinopsis spp.

Remarks: This group constitutes several new species, to be formally described elsewhere.

Reticulosphaera actinocoronata

Samlandia chlamydophora

Schematophora speciosa

Selenopemphix spp.

Spinidinium luciae (see Sluijs and Brinkhuis, submitted [N3] for comments)

Spinidinium macmurdoense (see Sluijs and Brinkhuis, submitted [N3] for comments)

Spinidinium spp. (pars.)

Remarks: This group constitutes several new species that are formally described in Sluijs and Brinkhuis, submitted [N3].

Spiniferites spp.

Stoveracysta kakanuiensis

Stoveracysta ornata

Tectatodinium spp.

Thalassiphora pelagica

Turbiosphaera filosa

Vozzhennikovia spp.

Remarks: This group constitutes several new species that are formally described in Sluijs and Brinkhuis, submitted [N3].

Wilsonidinium ornatum

Figure F1. ODP Leg 189 drilling locations (Sites 1168–1172).

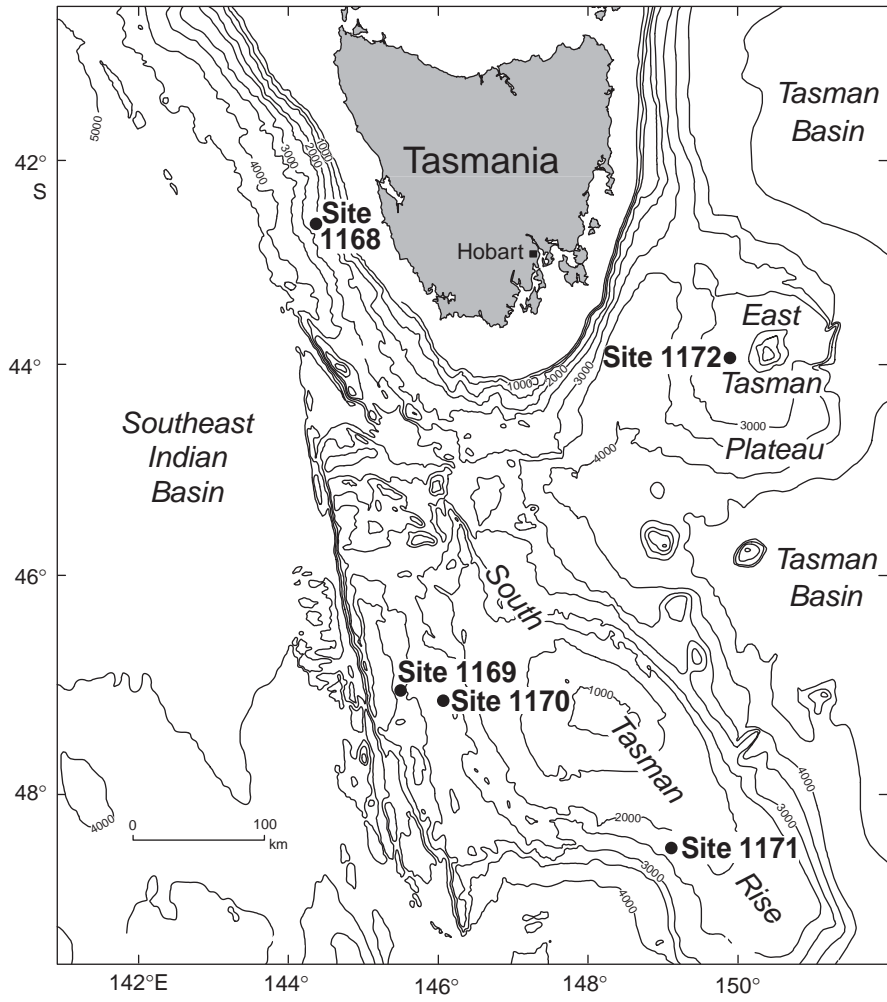


Figure F2. Dinocyst assemblage distribution through the Eocene–Oligocene transition among ODP Leg 189 Sites 1170–1172. Dinocyst association 1 = Antarctic-endemic, marginal marine, and eutrophic; association 2 = more cosmopolitan and more open marine; association 3 = coastal upwelling, open marine. For species composition and paleoecological discussion, see text. Lithologic units are from Exxon, Kennett, Malone, et al. (2001).

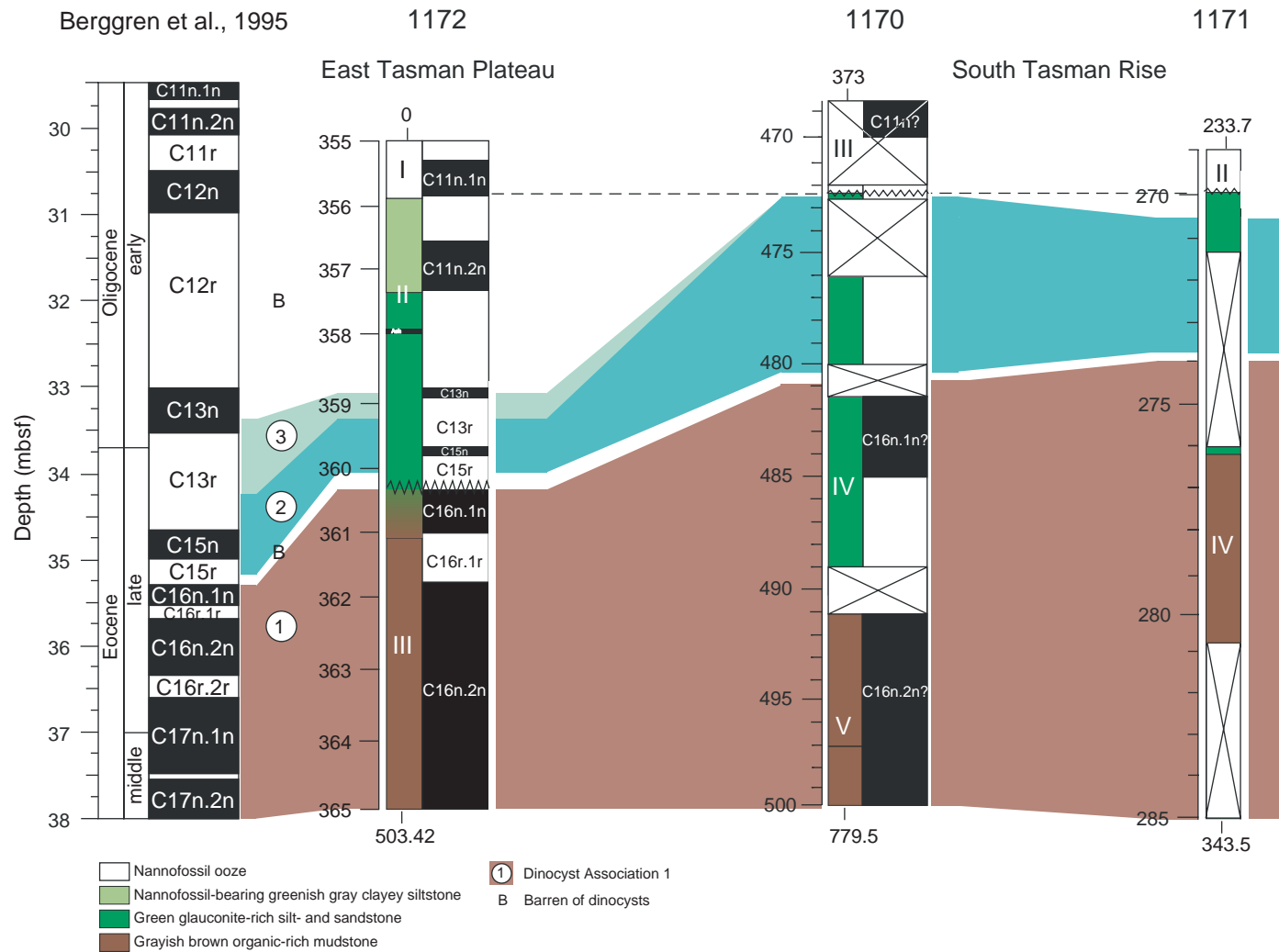


Figure F3. Correlation of the Eocene–Oligocene transition among ODP Leg 189 Sites 1168 and 1170–1172 based on qualitative and quantitative dinocyst information, diatom events, and magnetostratigraphy. *A.verr* = *Aireiana verrucosa*, *A.dist* = *Alterbidinium distinctum*, *Brig?* = *Brigantedinium?* sp., *C.plac* = *Cleistosphaeridium placacanthum*, *D.ant* = *Deflandrea antarctica* group, *D.sp.A* = *Deflandrea* sp. A, *H.sem* = *Hemiplacophora semilunifera*, *H.cf.oc* = *Hystrichokolpoma* sp. cf. *Homotryblium oceanicum*, *P.ech* = *Phthanoperidinium echinatum* group, *S.spec* = *Schematophora speciosa*, *Spin* = *Spinidinium* spp., *S.kak* = *Stoveracysta kakanuiensis*, *S.orn* = *Stoveracysta ornata*, *T.fil* = *Turbiosphaera filosa*, *Paly* = palynomorphs, *H.car* = *Hemiaulus characteristicus*, *D.arch* = *Distephanosira architecturalis*, *R.vig (s)* = *Rocella vigilans* (small), *C.jous* = *Cavitatus jouseanus*. LO = last occurrence, FO = first occurrence. Lithologic units are from Exon, Kennett, Malone, et al. (2001).

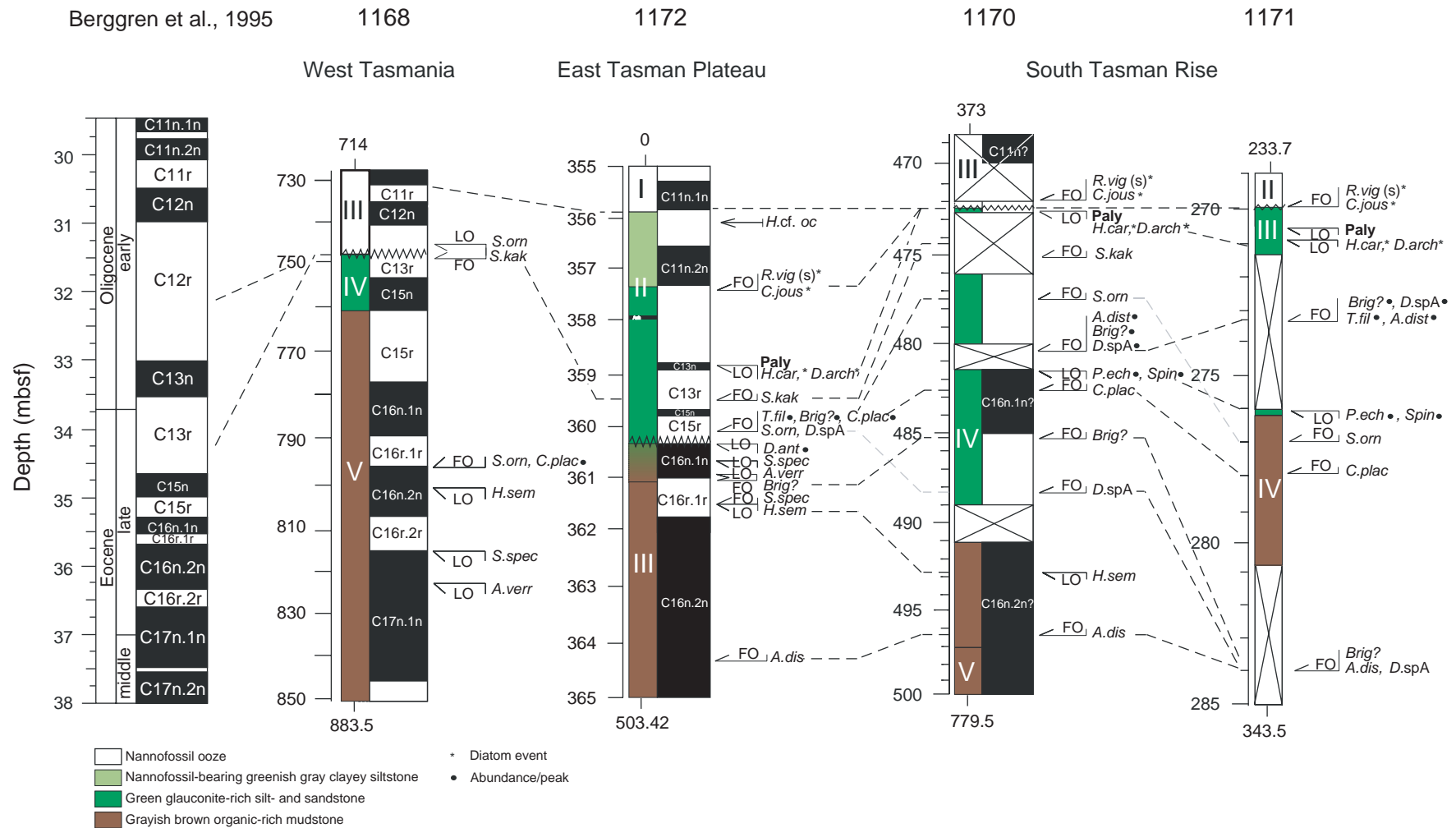


Figure F4. Correlation of Hole 1171C to Hole 1171D using (corrected) magnetic susceptibility (MS). Note that the offset between the two holes is 3.6 m and that we use 1171D mbsf for plotting. Alternatively, [Stickley et al.](#) (this volume) correlated Hole 1171D to Hole 1171C and use Hole 1171C mbsf, resulting in a 7.2-m offset between the 1171 mbsf in this paper vs. that shown in [Stickley et al.](#) (this volume).

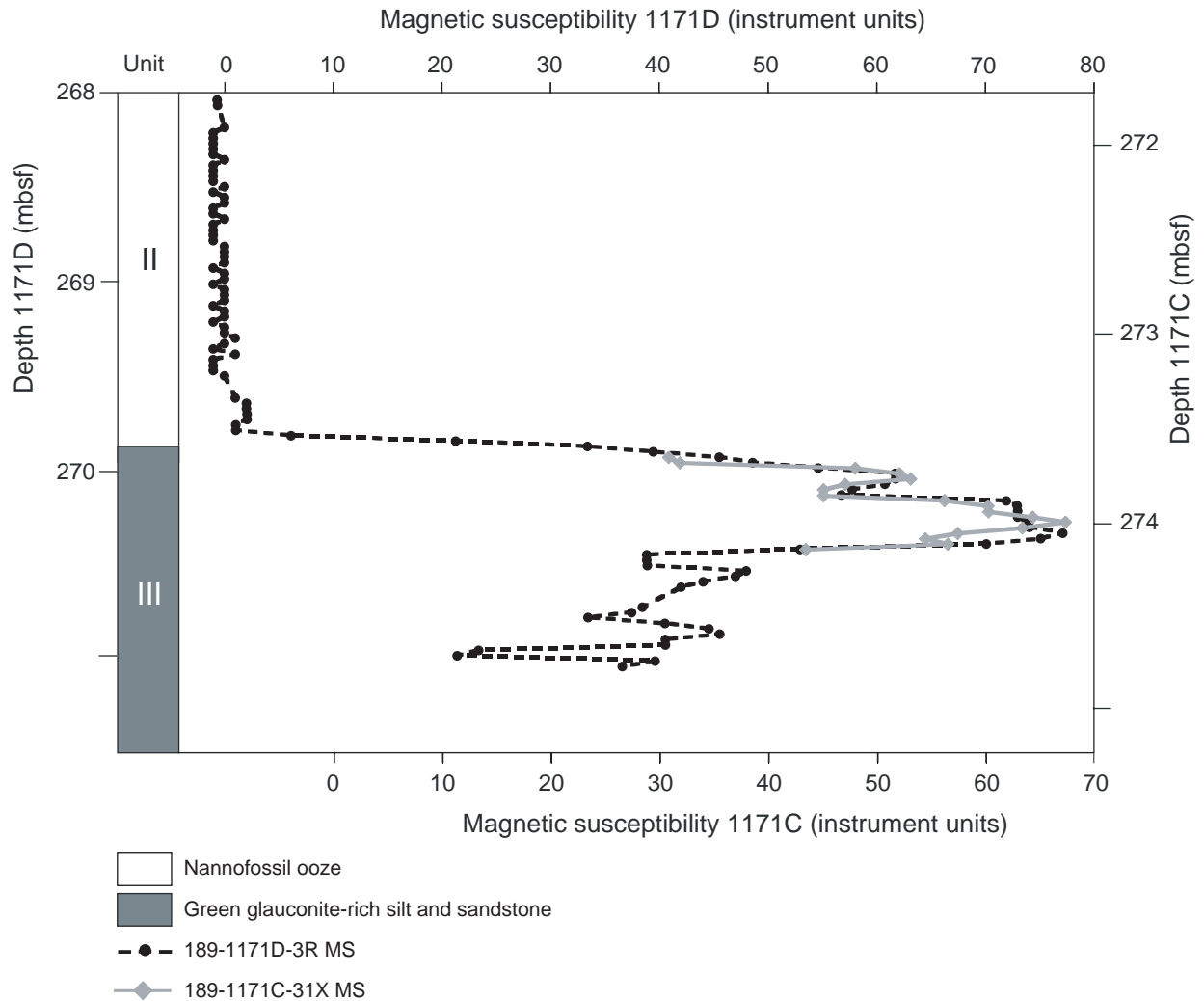


Table T1. Palynological results from samples of Hole 1170D. (Continued on next page.)

Core, section, interval (cm)	Median depth (mbsf)	N (palytomorphs)	N (dinocysts)	N (sporomorphs)	N (foram linings)	N (acritarchs)	Cysts per gram	Unit	Association	<i>Alterbidinium distinctum</i>	<i>Alterbidinium/Senegalium</i> spp.	<i>Batiacasphaera</i> spp.	<i>Brigantedinium?</i> sp.	<i>Cerebrocysta/Pyxidinopsis</i> spp.	<i>Cleistosphaeridium</i> spp.	<i>Cooksonidium capricornum</i>	<i>Cordosphaeridium minimum</i>	<i>Corrudinium</i> spp.	<i>Deflandrea antarctica</i> group	<i>Deflandrea convexa</i> group	<i>Deflandrea phosphoritica</i> group	<i>Deflandrea</i> sp. A	<i>Deflandrea</i> indet.	<i>Diphyes colligerum</i>	<i>Echinidinium</i> spp.	<i>Elytrocysta</i> spp.	<i>Enneadocysta partridgei</i>	<i>Enneadocysta</i> sp. A	<i>Hemiplacophora semilunifera</i>	
189-1170D-																														
6R-1, 34-36	472.24	0	0	0	0	0	0	Pel	B																					
6R-CC,16-19	472.80	352	230	43	4	75	4,000	Tra	2	7		2	11	1	1.5	1					3.5	7	6.5		1	2	2	1		
7R-1, 0-2	476.62	358	300	22	0	36	6,000	Tra	2	65		1	2	1						2	4	8.5	9.5		3		3			
7R-1, 25-27	476.87	225	144	50	2	29	2,000	Tra	2	13			5	2	1						8	6	1.5		3		5	1		
7R-1, 50-52	477.12	387	247	81	3	56	4,000	Tra	2	21			10	2							1	8	7		2		5			
7R-1, 75-77	477.37	319	201	72	2	44	3,000	Tra	2	21.5		1	7		2	3	4				3	8	8		2	1	3	2		
7R-1, 85-87	477.47	320	167	53	6	94	4,000	Tra	2	9.5	1	2	10	4	1	2	2				3	5.5	4.5				2.5			
7R-2, 85-87	478.97	280	177	65	15	23	8,000	Tra	2	6			6	5		3	2				1	10	3				3	1		
8R-1, 85-87	482.37	903	770	103	13	17	37,000	Tra	1	4		1	8	2	1	1	7	1	3		5	6	10				4			
8R-2, 85-87	483.87	348	255	46	7	40	12,000	Tra	1	5			5			3	1	2			2	1	8.5				2			
8R-3, 85-87	485.37	482	342	68	11	61	16,000	Tra	1	8		2	2	2		4		1			10	1	6.5				6	2		
8R-4, 85-87	486.87	413	322	37	6	48	15,000	Tra	1	3				1		1					5	4		1			4			
8R-5, 82-84	488.34	413	325	45	5	38	22,000	Tra	1	2						6					19	3	4.25				12			
9R-1, 85-87	491.97	399	329	16	2	52	23,000	Spd	1		1					4					40		1				2	2		
9R-2, 85-87	493.47	499	315	33	15	136	15,000	Spd	1	1.5				1		10					1						5	1	1	
9R-3, 85-87	494.97	325	201	39	13	72	10,000	Spd	1	1						2			2		1						6			
9R-4, 85-87	496.47	293	183	31	5	74	9,000	Spd	1	1						5	2				1	0.5					6	1		

Notes: N = number. Pel = pelagic, Tra = transitional, Spd = siliciclastic pro-deltaic. B = barren.

Table 1 (continued).

Core, section, interval (cm)	Median depth (mbsf)	<i>Hystrichosphaeridium rigaudiae</i>	<i>Hystrichosphaeridium truswelliae</i>	<i>Impagidinium</i> spp.	<i>Lejeunecysta</i> spp.	<i>Nematosphaeropsis labyrinthus</i>	<i>Octodinium askiniae</i>	<i>Operculodinium</i> spp.	<i>Paucisphaeridium</i> spp.	<i>Phthanoperidinium echinatum</i> group	<i>Samlandia chlamydothora</i>	<i>Selenopemphix</i> spp.	<i>Spinidinium colemanii</i>	<i>Spinidinium luciae</i>	<i>Spinidinium macmurdoense</i>	<i>Spiniferites</i> spp.	<i>Stoveracysta kakaniensis</i>	<i>Stoveracysta ornata</i>	<i>Tectatodinium</i> spp.	<i>Turbiosphaera filosa</i>	<i>Vozzhemikovia</i> spp.	Dinocysts indet.	
189-1170D- 6R-1, 34-36	472.24																						
6R-CC,16-19	472.80	1	3	1	1		16	2	12	28		20.5	2		8	3	4			1	59	26	
7R-1, 0-2	476.62		2	2	1		24	3		48		6	1	10	2					6	86	14	
7R-1, 25-27	476.87		3	6	1		17	7	1	18		6	1	1	1					3.5	19	11	
7R-1, 50-52	477.12		5	8			11	11	3	61		12		9	6					0.5	34	23	
7R-1, 75-77	477.37		4	3			12	11		31		6	1	11	2					4	33	14	
7R-1, 85-87	477.47		5	7			10	6	5	27		10	2		8	1			1	1	18	19	
7R-2, 85-87	478.97				2		1	3		20		5	17	1	3	3					78.5	3	
8R-1, 85-87	482.37		2	1	1		5	18		386		6	118	3	22	11				19	117	8	
8R-2, 85-87	483.87		5.5				4	9	1	68.5		1	9		23	4				9	86	5	
8R-3, 85-87	485.37		1.5	1			15.5	8	4	95		9	5	1	61					3.5	89.5	3	
8R-4, 85-87	486.87		1	0.5			4	3		166		1			11	1				15	100		
8R-5, 82-84	488.34		1	3	2		5	11		90	2	9			43.5	5.5				18	87	2	
9R-1, 85-87	491.97		1	1			14	5		171		4		1	20	5				5	46	2	
9R-2, 85-87	493.47		1	3	3		6		2	28		3			50	2				5	185	6	
9R-3, 85-87	494.97			1.5	3		5			38		10			40.5	3				3	82.5	2	
9R-4, 85-87	496.47		2.5	0.5	3		12	5		21		12			16	4				1	83	6	

Table T2. Palynological results from samples of Hole 1171D. (Continued on next page.)

Core, section, interval (cm)	Median depth (mbsf)	N palynomorphs	N dinocysts	N sporomorphs	N foram linings	N acritarchs	Cysts per gram	Unit	Association	<i>Alterbidinium distinctum</i>	<i>Batiacasphaera</i> spp.	<i>Brigantedinium?</i> sp.	<i>Cerebrocysta/Pyxidiniopsis</i> spp.	<i>Cleistosphaeridium</i> spp.	<i>Cordosphaeridium minimum</i>	<i>Corrudinium</i> spp.	<i>Deflandrea antarctica</i> group	<i>Deflandrea cygniformis</i>	<i>Deflandrea phosphorica</i> group	<i>Deflandrea</i> sp. A	<i>Deflandrea</i> indet.	<i>Echinidinium</i> spp.	<i>Elytrocysta</i> spp.	<i>Enneadocysta partridgei</i>
189-1171D-																								
3R-1, 85-87	267.46	0	0	0	0	0	0	Pel	B															
3R-2, 30-32	268.41	0	0	0	0	0	0	Pel	B															
3R-2, 85-87	268.96	0	0	0	0	0	0	Pel	B															
3R-2, 105-107	269.16	0	0	0	0	0	0	Pel	B															
3R-3, 5-7	269.66	0	0	0	0	0	0	Pel	B															
3R-3, 30-32	269.91	0	0	0	0	0	0	Pel	B															
3R-3, 55-57	270.16	0	0	0	0	0	0	Pel	B															
3R-3, 80-82	270.41	0	0	0	0	0	0	Pel	B															
3R-3, 105-107	270.66	400	291.5	28	4	75	7000	Tra	2	20.5	36	5	6	2	3		2	6	25	11	3	6	18	
3R-4, 13-15	270.90	334	250.5	15	6	61	5000	Tra	2	8.5	1	16	2	4	3.5	1	1	6	1	8		1	16	
3R-4, 38-40	271.15	317	239.5	17	6	52	5000	Tra	2	7.5		10	1	1	2			4	14.5	9	1	5	8	
4R-1, 55-57	276.76	542	212	21	5	301	7000	Spd	1				1		1.5			2		4		3	10	
4R-1, 105-107	277.26	303	154	20	6	123	5000	Spd	1	7	1		1	2	1			3	3	3			5	
4R-2, 5-7	277.76	487	282.5	24	8	171	9000	Spd	1	5	3	4	1	5	5			8	2	5.5			13	
4R-2, 55-57	278.26	500	309	26	12	153	9000	Spd	1	3	2			4	1			4	1	4		3	6	

Notes: N = number. Pel = pelagic, Tra = transitional, Spd = siliciclastic pro-deltaic. B = barren.

Table T2 (continued).

Core, section, interval (cm)	Median depth (mbsf)	<i>Enneadocysta</i> sp. A	<i>Gelatia inflata</i>	<i>Hystriocholpoma rigaudiae</i>	<i>Impagidinium</i> spp.	<i>Lejeunecysta</i> spp.	<i>Lingulodinium machaerophorum</i>	<i>Nematosphaeropsis labyrinthus</i>	<i>Octodinium askirinae</i>	<i>Operculodinium</i> spp.	<i>Paucisphaeridium</i> spp.	Phthanoperidinium echinatum group	<i>Samlandia chlamydothora</i>	<i>Selenopemphix</i> spp.	<i>Senegalinium asymmetricum</i>	<i>Spinidinium colemanii</i>	<i>Spinidinium luciae</i>	<i>Spinidinium macmurdoense</i>	<i>Spinidinium</i> indet.	<i>Spiniferites</i> spp.	<i>Stoveracysta ornata</i>	<i>Tectatodinium pellitum</i>	<i>Thalassiphora pelagica</i>	<i>Turbiosphaera filosa</i>	<i>Vozzhennikovia</i> spp.	Dinocysts indet.
189-1171D-																										
3R-1, 85–87	267.46																									
3R-2, 30–32	268.41																									
3R-2, 85–87	268.96																									
3R-2, 105–107	269.16																									
3R-3, 5–7	269.66																									
3R-3, 30–32	269.91																									
3R-3, 55–57	270.16																									
3R-3, 80–82	270.41																									
3R-3, 105–107	270.66	2		14	16			29	4	3		11	14				1	6	2			1	4	34	7	
3R-4, 13–15	270.90	1	2	8	5			14	9	23		12	8					1	1	4			15	75	17	
3R-4, 38–40	271.15	2		1	5			1	9	6	6	65	1	3	3			1	3	3		1	15.5	39	12	
4R-1, 55–57	276.76			1	1			10	11	4		132	2					1	1	55	1		1	15	5	
4R-1, 105–107	277.26			55	4	05		18	9	4		67	5					6	1					7	1	
4R-2, 5–7	277.76	1		10	1			34	1	4		110	9					13	3	1			3	25	14	
4R-2, 55–57	278.26	2	1	6	8		2	29	8	6		119	2		1			12		8			3	62	12	

Table T3. Palynological results from samples of Hole 1172A. (See table notes. Continued on next five pages.)

Core, section, interval (cm)	Median Depth	N (palyomorphs)	N (dinocysts)	N (sporomorphs)	N (foram linings)	N (acritarchs)	Cysts per gram	Unit	Association	<i>Achomospaera</i> <i>alcicornu</i>	<i>Achomospaera</i> <i>ramulifera</i>	<i>Aireiana</i> <i>verrucosa</i>	<i>Alterbidinium</i> <i>distinctum</i>	<i>Alterbidinium</i> / <i>Senegalinium</i> spp.	<i>Areoligera</i> <i>semicirculata</i> ?	<i>Batiacasphaera</i> spp.	<i>Brigantidinium</i> ? sp.	<i>Cerebrocysta</i> / <i>Pyxidiniopsis</i> spp.	<i>Cleistosphaeridium</i> spp.	<i>Cordosphaeridium</i> <i>fibrospinosum</i>	<i>Cordosphaeridium</i> <i>minimum</i>	
189-1172A-																						
38X-CC, 24-29	353.67	0	0	0	0	0	0	Pel	B													
39X-2, 3-5	356.14	172	167	0	1	4		Pel						1			4					
39X-2, 135-137	356.29	0	0	0	0	0	0	Pel	B													
39X-2, 10-12	357.46	0	0	0	0	0	0	Pel	B													
39X-3, 42-44	357.71	0	0	0	0	0	0	Pel	B													
39X-3, 61-63	358.03	0	0	0	0	0	0	Pel	B													
39X-3, 74-76	358.22	0	0	0	0	0	0	Pel	B													
39X-3, 85-87	358.35	0	0	0	0	0	0	Pel	B													
39X-3, 100-102	358.46	0	0	0	0	0	0	Pel	B													
39X-3, 105-107	358.61	0	0	0	0	0	0	Pel	B													
39X-3, 118-120	358.66	0	0	0	0	0	0	Pel	B													
39X-3, 122-124	358.79	419	385	13		21	6,000	Tra	3				1				294	2	3		1	
39X-3, 128-130	358.83	298	280	8		10		Tra	3								220			1		
39X-3, 138-140	358.89	380	292	54		34	4,000	Tra	3								158	2	1	3		
39X-3, 145-147	358.99	418	260	88	1	69	6,000	Tra	3								58	5	1	1		
39X-3, 148-150	359.06	222	153	37	2	30		Tra	3		2	1		1			49	1	2	2		
39X-3, 5-7	359.09	221	133	41	4	43	2,000	Tra	3								22	6		1		
39X-4, 10-12	359.16	284	211	41	3	29		Tra	3				1				12		4	1	10	
39X-4, 14-16	359.21	207	149	35	2	21		Tra	3				1	1			16	1	12	1		
39X-4, 25-27	359.25	432	257	108	3	64	2,000	Tra	3						4		48	8	14.5		1	
39X-4, 30-32	359.36	209	124	45	5	35		Tra	2				1				13		12			
39X-4, 40-42	359.41	246	125	89	2	30	2,000	Tra	2								6	2	6	1	3	
39X-4, 44-46	359.51	241	189	29	3	20		Tra	2								29		9	1		
39X-4, 45-47	359.55	405	250	100	1	54	3,000	Tra	2		1				3		12	2	14		1	
39X-4, 60-62	359.56	208	135	35	3	35		Tra	2		1						20	1	6			
39X-4, 65-67	359.71	605	330	212		63	3,000	Tra	2								1	12	8	1	1	2
39X-4, 74-76	359.76	247	155	75	2	15		Tra	2								15			1		
39X-4, 85-87	359.85	386	278	75	1	32	3,000	Tra	2						4		15	10	1		2	
39X-4, 90-92	359.96	115						Tra	2								10	1	2			
39X-4, 104-106	360.01	460	291	113		56	3,000	Tra	2				6.5		2		26	10	1			
39X-4, 120-122	360.15	0	0	0	0	0	0		B													
39X-4, 130-132	360.31	0	0	0	0	0	0		B													
39X-4, 134-136	360.41	267	237	20		10		Spd	1	1	1			1								
39X-4, 146-150	360.45	498	274	171	1	52	4,000	Spd	1								1	6			1	

Table T3 (continued).

Core, section, interval (cm)	Median Depth	<i>Corrudinium</i> spp.	<i>Dapsilidinium pseudocolligerum</i>	<i>Deflandrea antarctica</i> group	<i>Deflandrea phosphoritica</i> group	<i>Deflandrea</i> sp. A	<i>Dinopterigium cladooides</i>	<i>Diphyes colligerum</i>	<i>Distatodinium</i> spp.	<i>Elytrocysta</i> spp.	<i>Enneadocysta partridgei</i>	<i>Enneadocysta pectiniformis</i>	<i>Enneadocysta</i> sp. A	<i>Eocladopyxis</i> spp.	<i>Gelatia inflata</i>	<i>Glaphrocysta intricata</i>	<i>Hemiplacophora semilunifera</i>	<i>Histiocysta</i> sp.	<i>Hystrichokolpoma rigaudiae</i>	<i>Hystrichokolpoma</i> sp. cf. <i>Homotryblum oceanicum</i>	<i>Hystrichosphaeropsis</i> spp.	<i>Hystrichostrogylon</i> spp.	<i>Impagidinium</i> spp.
189-1172A-																							
38X-CC, 24-29	353.67																						
39X-2, 3-5	356.14		1		1				1	1		1				2			35	1	15		1
39X-2, 135-137	356.29																						
39X-2, 10-12	357.46																						
39X-3, 42-44	357.71																						
39X-3, 61-63	358.03																						
39X-3, 74-76	358.22																						
39X-3, 85-87	358.35																						
39X-3, 100-102	358.46																						
39X-3, 105-107	358.61																						
39X-3, 118-120	358.66																						
39X-3, 122-124	358.79				1	21.75				1	2.5												1
39X-3, 128-130	358.83			5	2	22												1					1
39X-3, 138-140	358.89				2	20.5				1	1				1								2
39X-3, 145-147	358.99				2	8.25		1		18	1								1				6
39X-3, 148-150	359.06			4	3	8			2	1	4		1					1	1				1
39X-3, 5-7	359.09				1	7				12	2								2				6
39X-4, 10-12	359.16	3	2	4	16	10					5								5				7
39X-4, 14-16	359.21	1		6	4	7					4								3				3
39X-4, 25-27	359.25	2.5			3	6				38	1				2			1	1				7.5
39X-4, 30-32	359.36	2		3	2	10					1							1	1				3
39X-4, 40-42	359.41	1			2	3				9								3					6
39X-4, 44-46	359.51	4		4	1	20				1	2							1	7				3
39X-4, 45-47	359.55	4			1	5				17	1								3				7
39X-4, 60-62	359.56			2	1	9					1				1			1	4				4
39X-4, 65-67	359.71	6			4.5	6				18	1							1	4.5				14.5
39X-4, 74-76	359.76	2		2	15	5				3	2	1						1	1				3
39X-4, 85-87	359.85	3		1	8	13.5	1			8	1							3					3.5
39X-4, 90-92	359.96			10	4	6					2							1					3
39X-4, 104-106	360.01	7		2	10	3.5				10	4							2	0.5				17
39X-4, 120-122	360.15																						
39X-4, 130-132	360.31																						
39X-4, 134-136	360.41	2		200	13						2		1						1				2
39X-4, 146-150	360.45	1		145	9					1	13												8

Table T3 (continued).

Core, section, interval (cm)	Median Depth	<i>Lejeunecysta</i> spp.	<i>Lingulodinium machaerophorum</i>	<i>Melitasphaeridium pseudorecurvatum</i>	<i>Nematosphaeropsis labyrinthus</i>	<i>Octodinium askiniae</i>	<i>Operculodinium</i> sp. A	<i>Operculodinium</i> spp.	<i>Palaeocystodinium</i> spp.	<i>Paucisphaeridium</i> spp.	<i>Phtharoperidinium echinatum</i> group	<i>Reticulatosphaera actinocoronata</i>	<i>Samlandia chlamydophora</i>	<i>Schematophora speciosa</i>	<i>Selenopemphix</i> spp.	<i>Spinidinium</i> spp.	<i>Spiniferites</i> spp.	<i>Stoveracysta kakanuiensis</i>	<i>Stoveracysta ornata</i>	<i>Tectatodinium</i> spp.	<i>Thalassiphora pelagica</i>	<i>Turbiosphaera filosa</i>	<i>Vozzhennikovia</i> spp.	<i>Wilsonidinium ornatum</i>
189-1172A-																								
38X-CC, 24–29	353.67																							
39X-2, 3–5	356.14		1					17			1	4					80							
39X-2, 135–137	356.29																							
39X-2, 10–12	357.46																							
39X-3, 42–44	357.71																							
39X-3, 61–63	358.03																							
39X-3, 74–76	358.22																							
39X-3, 85–87	358.35																							
39X-3, 100–102	358.46																							
39X-3, 105–107	358.61																							
39X-3, 118–120	358.66																							
39X-3, 122–124	358.79	1							1	1	25					16	2	3					0.5	7
39X-3, 128–130	358.83		4						1		10					3	3	2					1	1
39X-3, 138–140	358.89	2	8			3				3	48				5	18	7	1					1	4
39X-3, 145–147	358.99	7	4		1	4				3	15	50	2		4	5	15.5	15.5	2					29
39X-3, 148–150	359.06	5	2			1			1		7	1			2	6	21	1			1	2		19
39X-3, 5–7	359.09	1				6				2	12	8			5	3	9	4	1					21
39X-4, 10–12	359.16	1	2			1		19			2	1	2		4	4	63	28			1	2		4
39X-4, 14–16	359.21	1	1			7		5			10	1			3		46	2				8		5
39X-4, 25–27	359.25	6	1			5		1	2	14	31		1		2	2.5	31	4	1	4	0.5	1		10
39X-4, 30–32	359.36	4	1			15		3			7				2	1	29					5		8
39X-4, 40–42	359.41	2				7		2	1	5	12				3	2.5	18.5	1						22
39X-4, 44–46	359.51	20	1			10		11			7		1		2		12	2			1	2		34
39X-4, 45–47	359.55	2	3			4		2	12	17	15					3	14			2		2		99
39X-4, 60–62	359.56	12	1			11		3			6				3		14					1		32
39X-4, 65–67	359.71	2	4			5			6	14	46				7	2	26.5					9		115
39X-4, 74–76	359.76	5	1			9		4			11				2	4	14					25		22
39X-4, 85–87	359.85	3				12		2	7	5	38				10	7	19.5		1			14		72
39X-4, 90–92	359.96	2	1			3		2			3				1	6	10		2		2	37		
39X-4, 104–106	360.01	2	5			8		2	21	14	47				1	2	69		2	1		1		14
39X-4, 120–122	360.15																							
39X-4, 130–132	360.31																							
39X-4, 134–136	360.41		1			1		1			5					2	1							1
39X-4, 146–150	360.45	2	1			6			3	18	22				8	12	3							13

Table T3 (continued).

Core, section, interval (cm)	Median Depth	N (palytomorphs)	N (dinocysts)	N (sporomorphs)	N (foram linings)	N (acritarchs)	Cysts per gram	Unit	Association	<i>Achomosphaera</i> <i>alcicornu</i>	<i>Achomosphaera</i> <i>ramulifera</i>	<i>Aireiana</i> <i>verrucosa</i>	<i>Alterbidinium</i> <i>distinctum</i>	<i>Alterbidinium</i> / <i>Senegalinium</i> spp.	<i>Areoligera</i> <i>semicirculata</i> ?	<i>Batiacasphaera</i> spp.	<i>Brigantidinium</i> ? sp.	<i>Cerebrocysta</i> / <i>Pyxidiniopsis</i> spp.	<i>Cleistosphaeridium</i> spp.	<i>Cordosphaeridium</i> <i>fibrospinosum</i>	<i>Cordosphaeridium</i> <i>minimum</i>
39X-4, 147-149	360.57	354	284	49	1	20	8,000	Spd	1				2.5	1							1
39X-4, 5-7	360.58	230	189	30	1	10		Spd	1	1	1						1				
39X-5, 10-12	360.66	205	190	8	0	7		Spd	1												1
39X-5, 17-19	360.71	221	198	20	1	2		Spd	1	1							2				
39X-5, 22-24	360.78	216	188	19	2	7		Spd	1	1	1										
39X-5, 28-30	360.83	181	157	10	1	13		Spd	1	1	1						1				
39X-5, 44-46	360.89	759	692	29	4	34	15,000	Spd	1			1	5	2			9	1			2
39X-5, 55-57	361.05	505	447	39	1	18	20,000	Spd	1				35	2			2				
39X-5, 85-87	361.16	378	357	12		9		Spd	1			2	1								2
39X-5, 100-102	361.46	340	323	5	1	11		Spd	1				10	18							1
39X-5, 105-107	361.61	139	123	12	1	3		Spd	1	1	1		1	1							
39X-5, 5-7	361.66	262	249	4	2	7		Spd	1				13	30							2
39X-6, 10-12	362.16	169	133	25	6	5		Spd	1	1	1		1	1			1	1			
39X-6, 55-57	362.21	129	108	18	1	2		Spd	1				2	1			0			1	
39X-6, 64-66	362.66	341	322	12	1	6		Spd	1				1	1			1				
39X-6, 85-87	362.75	221	210	4	1	6		Spd	1				1	5							
39X-6, 100-102	362.96	332	322	4	2	4		Spd	1				7	10			1			1	1
39X-6, 105-107	363.11	197	179	7	1	10		Spd	1		1										
39X-6, 122-124	363.16	297	279	12	1	5		Spd	1				8	10							3
39X-6, 142-144	363.33	167	144	9	5	9		Spd	1				5	24						1	
39X-6, 5-7	363.53	139	136	1	1	1		Spd	1					1						1	
39X-7, 10-12	363.66	169	167	1	1			Spd	1				1								
39X-7, 31-33	363.71	171	166	4		1		Spd	1				1	1							
39X-7, 40-42	363.92	121	110	8		3		Spd	1					1							
39X-7, 45-47	364.01	135	113	16	1	5		Spd	1					1							
39X-7, 27-33	364.06	138	129	4	1	4		Spd	1				1	2							
39X-CC, 85-87	364.24	222	207	8	6	1		Spd	1				1	2							
40X-1, 85-87	365.06	269	239	18	3	9		Spd	1					4			3				3
40X-2, 85-87	366.56	238	230	3	0	5		Spd	1					1							
40X-3, 85-87	368.06	335	324	8	0	3		Spd	1					4							1
40X-4, 85-87	369.56	291	283	4	1	3		Spd	1					2							6
40X-5, 85-87	371.06	252	235	9	2	6		Spd	1								2				1
40X-6, 85-87	372.56	342	341	1	0	0		Spd	1								1				1
40X-CC, 26-31	373.90	238	217	7	11	3		Spd	1					10							
41X-1, 85-87	374.66	218	192	18	0	8		Spd	1					1	1		3				
41X-5, 86-88	380.52	278	253	13	1	11		Spd	1								1				2

Notes: N = number. Pel = pelagic, Tra = transitional, Spd = siliciclastic pro-deltaic. B = barren.

Table T3 (continued).

Core, section, interval (cm)	Median Depth	<i>Corrudinium</i> spp.	<i>Dapsilidinium pseudocollegerum</i>	<i>Dellandrea antarctica</i> group	<i>Dellandrea phosphoritica</i> group	<i>Dellandrea</i> sp. A	<i>Dinopterigium cladoides</i>	<i>Diphyes colligerum</i>	<i>Distatodinium</i> spp.	<i>Elytrocysta</i> spp.	<i>Enneadocysta partridgei</i>	<i>Enneadocysta pectiniformis</i>	<i>Enneadocysta</i> sp. A	<i>Eocladopyxis</i> spp.	<i>Gelatia inflata</i>	<i>Glaphrocysta intricata</i>	<i>Hemiplacophora semilunifera</i>	<i>Histocysta</i> sp.	<i>Hystriehokolpoma rigaudiae</i>	<i>Hystriehokolpoma</i> sp. cf. <i>Homotryblium oceanicum</i>	<i>Hystriehosphaeropsis</i> spp.	<i>Hystriehostroglylon</i> spp.	<i>Impagidinium</i> spp.
39X-4, 147–149	360.57	1		187	19						11							2					3
39X-4, 5–7	360.58	1		124	18						4		1	1				1					3
39X-5, 10–12	360.66	7		150	13						4			1									2
39X-5, 17–19	360.71	4		153	10						1								3				2
39X-5, 22–24	360.78	1	1	130	6					1	5					1			1				1
39X-5, 28–30	360.83	2	1	70	7						5					1			1				2
39X-5, 44–46	360.89	3		566	2						2							1	2				5
39X-5, 55–57	361.05	1		310	11					1	1							1	2				2
39X-5, 85–87	361.16	9		221	10						2							1	1				11
39X-5, 100–102	361.46	4		144	21						4		1						1				2
39X-5, 105–107	361.61		1	40	5						1						1						0
39X-5, 5–7	361.66	2	2	68	9						3						1		1				4
39X-6, 10–12	362.16	1		66	2					1	5												1
39X-6, 55–57	362.21	2		51	4						5		1										3
39X-6, 64–66	362.66	5		200	7						3												16
39X-6, 85–87	362.75	2		55	3						1	1											3
39X-6, 100–102	362.96			239	15				2		4		1										9
39X-6, 105–107	363.11	2		75	15				1		1						1					1	3
39X-6, 122–124	363.16	4		105	6				1		8												23
39X-6, 142–144	363.33	2		30	5						2												3
39X-6, 5–7	363.53	1		70	12						1												4
39X-7, 10–12	363.66	2	1	121	25						1												1
39X-7, 31–33	363.71	2		90	18						1												1
39X-7, 40–42	363.92	2	1	9	1						2												1
39X-7, 45–47	364.01	2		22	3						33		1			1							2
39X-7, 27–33	364.06	2		20	4						42		9										1
39X-CC, 85–87	364.24	1		115	15					3	6	3											2
40X-1, 85–87	365.06	8		62	20						20		1	1									5
40X-2, 85–87	366.56	7		2	4						79					1							5
40X-3, 85–87	368.06	2		221	15						34			1					1				1
40X-4, 85–87	369.56	2		172	17						59								1				3
40X-5, 85–87	371.06	3		129	12						38												
40X-6, 85–87	372.56	1		315	9						10		1										1
40X-CC, 26–31	373.90			130	20					3	10												2
41X-1, 85–87	374.66	3		52	4				1		21								2				4
41X-5, 86–88	380.52	8	2	125	5				1		18	6				1							6

Table T3 (continued).

Core, section, interval (cm)	Median Depth	<i>Lejeunecysta</i> spp.	<i>Lingulodinium machaerophorum</i>	<i>Meliosphaeridium pseudorecurvatum</i>	<i>Nematosphaeropsis labyrinthus</i>	<i>Octodinium askiniae</i>	<i>Operculodinium</i> sp. A	<i>Operculodinium</i> spp.	<i>Palaeocystodinium</i> spp.	<i>Paucisphaeridium</i> spp.	<i>Phtharoperidinium echinatum</i> group	<i>Reticulatosphaera actinocoronata</i>	<i>Samlandia chlamydophora</i>	<i>Schematophora speciosa</i>	<i>Selenopemphix</i> spp.	<i>Spinidinium</i> spp.	<i>Spiniferites</i> spp.	<i>Stoveracysta kakanuiensis</i>	<i>Stoveracysta ornata</i>	<i>Tectatodinium</i> spp.	<i>Thalassiphora pelagica</i>	<i>Turbiosphaera filosa</i>	<i>Vozzhennikovia</i> spp.	<i>Wilsonidinium ornatum</i>
39X-4, 147-149	360.57	1				2			1	1	9				1	16	3							14
39X-4, 5-7	360.58	2	1			4		3			4				1	3	4					1	9	
39X-5, 10-12	360.66	1				1		2			3			1		3	3						5	
39X-5, 17-19	360.71	1				1		2			6				2	5	2						6	
39X-5, 22-24	360.78	1				1		1			10			1	7	2	5						10	
39X-5, 28-30	360.83	1	1			1		1			13			1	1	5	2						40	
39X-5, 44-46	360.89	2	1	1		4			3	4	9			1	1	11	4.5						50	
39X-5, 55-57	361.05					3			2	3	19				5	7	6						35	
39X-5, 85-87	361.16		1			2		6			1			3	2	33	13						36	
39X-5, 100-102	361.46		1			2		3			5			2	5	51	12			8			27	
39X-5, 105-107	361.61	1	1			3		1			4				3	32	1						25	
39X-5, 5-7	361.66		1			2		5			4				1	92	8						23	
39X-6, 10-12	362.16	2				5		2			7		1		1	5	7				1	1	19	
39X-6, 55-57	362.21	2				1		4	1		5				1	3					1		20	
39X-6, 64-66	362.66	2	2			1		3			2				1	69	6				1		25	
39X-6, 85-87	362.75	1				1		3			2				1	106	2					1	22	
39X-6, 100-102	362.96					11		3			7				2	2	5					1	12	
39X-6, 105-107	363.11	4				4		4			17				1	19	3					1	26	
39X-6, 122-124	363.16	2				23		4			12				3	21	9			1	1		34	
39X-6, 142-144	363.33	3				8		1			7				4	30	2				1		16	
39X-6, 5-7	363.53	1				15		1			10					9	1					1	8	
39X-7, 10-12	363.66					2		3			2				1	3	2						2	
39X-7, 31-33	363.71	2				3		4			9				1	16	2						15	
39X-7, 40-42	363.92					5		1			11				3	60	2					1	10	
39X-7, 45-47	364.01					5		5			10				1	14						2	11	
39X-7, 27-33	364.06	1				1		4			4				1	23	1					1	12	
39X-CC, 85-87	364.24	1				1		7			17				1	20	1						11	
40X-1, 85-87	365.06	2				14		19			21				2	30	6				1		17	
40X-2, 85-87	366.56	1				9		11	1		16				2	55	4				1		31	
40X-3, 85-87	368.06	2				4		3	1		7				2	1	4		2		1	1	16	
40X-4, 85-87	369.56	1				2		9			4						2				1		2	
40X-5, 85-87	371.06					2		15			13				1		7						12	
40X-6, 85-87	372.56																2							
40X-CC, 26-31	373.90	1				5		2			5					1	2					1	25	
41X-1, 85-87	374.66				1	6		12			19				1	3	23			1			34	1
41X-5, 86-88	380.52			1	1	2		10			22				3		21				1		17	

Plate P1. Illustrations of taxa, sample, and slide number. Scale bar = ~20 µm unless stated otherwise. Scanning electron microscope (SEM) photographs have varying scale bars. Many of the taxa below are also illustrated in [Brinkhuis, Sengers, et al.](#) (this volume). **1.** *Aireiana verrucosa* (Sample 189-1172A-39X-5, 55–57 cm) (1). **2.** *Alterbidinium distinctum* (Sample 189-1172A-39X-4, 85–87 cm) (2). **3, 4.** *Brigantedinium?* sp.; (3) Sample 189-1172A-39X-3, 122–124 cm (2) (scale bar = ~15 µm); note periphragm delineating long slender apical and antapical horns. (4) Sample 189-1172A-39X-3, 128–130 cm (2) (scale bar = ~15 µm); note periphragm delineating long slender antapical horns. **5.** *Deflandrea antarctica* group (Sample 189-1172A-39X-6, 85–87 cm) (1). **6.** *Deflandrea phosphoritica* group (Sample 189-1172A-39X-4, 10–12 cm) (1). **7.** *Deflandrea* sp. A (Sample 189-1170D-7R-2, 85–87 cm) (1). Note triangular endophragm. **8.** *Deflandrea* sp. A (Sample 189-1172A-39X-4, 74–76 cm) (1). Note triangular endophragm. **9.** *Enneadocysta partridgei* (Sample 189-1172A-39X-5, 105–107 cm) (1). **10.** *Enneadocysta* sp. A (Sample 189-1170D-7R-1, 25–27 cm) (1); note the two distally connected antapical processes. **11.** *Gelatia inflata* (Sample 189-1171D-4R-2, 55–57 cm) (1). **12.** *Octodinium askinia* (Sample 189-1171D-4R-2, 55–57 cm) (1). (Continued on next three pages.)

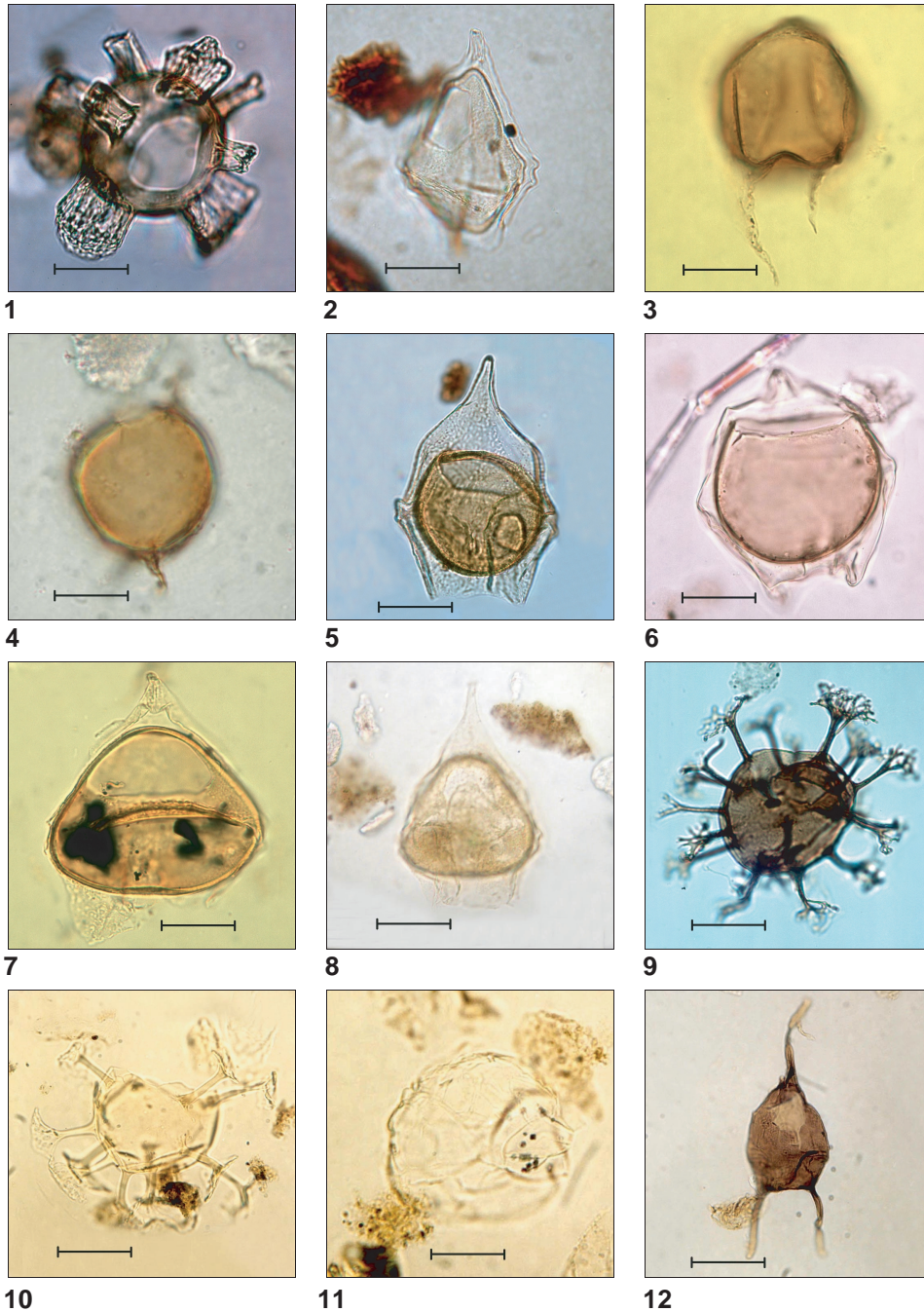
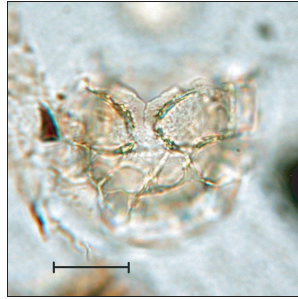


Plate P1 (continued). 13. *Paucisphaeridium* spp. (Sample 189-1172A-39X-4, 14–16 cm) (1); scale bar = ~10 μm . 14, 15. *Schematophora speciosa* (Sample 189-1172A-39X-5, 55–57 cm) (1); scale bar = ~15 μm . 16. *Spinidinium colemanii* (Sample 189-1170D-8R-1, 85–87 cm) (1). 17. *Spinidinium luciae* (Sample 189-1172A-39X-5, 55–57 cm) (1). 18. *Spinidinium macmurdoense* (Sample 189-1171D-4R-1, 105–107 cm) (1). 19, 20. *Stoveracysta kakanuiensis*; (19) Sample 189-1172A-39X-3, 122–124 cm (1); (20) Sample 189-1172A-39X-3, 145–147 cm (1). 21. *Turbiosphaera filosa* (Sample 189-1172A-39X-4, 10–12 cm) (1). 22. *Vozzhennikovia apertura* (Sample 189-1172A-39X-6, 85–87 cm) (1). 23, 24. *Vozzhennikovia?* spp. (Sample 189-1170D-8R-1, 85–87 cm) (1); note 3l archeopyle. (Continued on next page.)



13



14



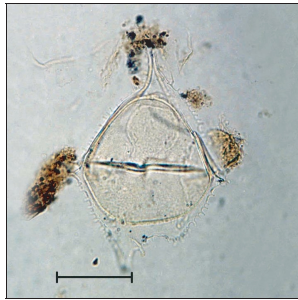
15



16



17



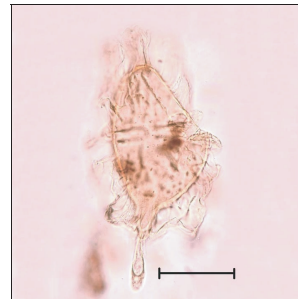
18



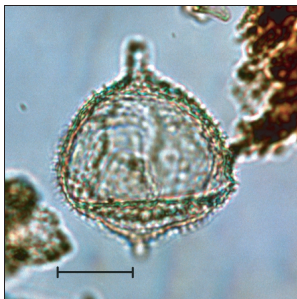
19



20



21



22



23

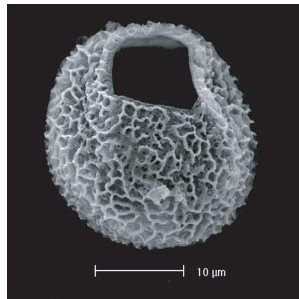


24

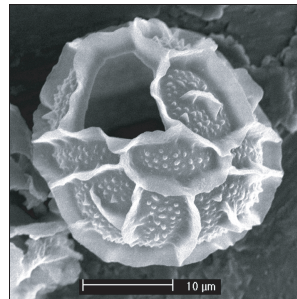
Plate P1 (continued). 25. *Vozzhennikovia?* spp. (Sample 189-1172A-39X-4, 44–46 cm) (1); note 3I archeopyle. 26. *Cerebrocysta* spp. (Sample 189-1172A-39X-4, 40–42 cm) (SEM). 27. *Corrudinium incompositum* (Sample 189-1172A-39X-3, 138–140) (SEM). 28. *Corrudinium* sp. Goodman and Ford, 1983 (Sample 189-1172A-39X-3, 138–140 cm) (SEM). 29, 30. *Deflandrea antarctica* (SEM); (29) Sample 189-1172A-39X-3, 48–50 cm; (30) Sample 189-1172A-39X-4, 147–149 cm. 31. *Deflandrea* sp. A (Sample 189-1172A-39X-4, 5–7 cm) (SEM). 32. *Enneadocysta partridgei* (Sample 189-1172A-39X-4, 147–149 cm) (SEM). 33. *Impagidinium disperitum* (Sample 189-1172A-39X-4, 147–149 cm) (SEM). 34. *Operculodinium* spp. (Sample 189-1172A-39X-4, 147–149 cm) (SEM). 35. *Phthanoperidinium echinatum* (Sample 189-1172A-39X-3, 138–140 cm) (SEM). 36. *Spinidinium luciae* (Sample 189-1172A-39X-6, 122–124 cm) (SEM). (Continued on next page.)



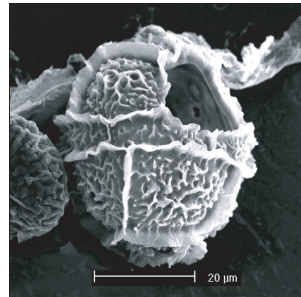
25



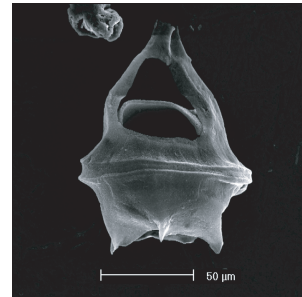
26



27



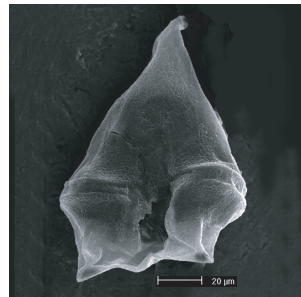
28



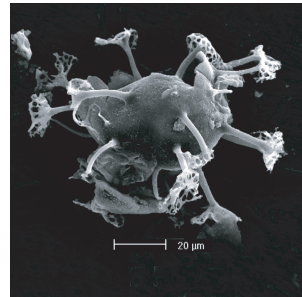
29



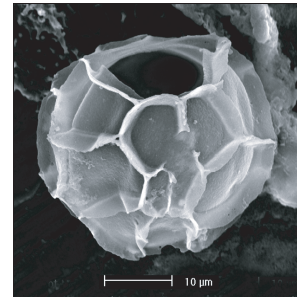
30



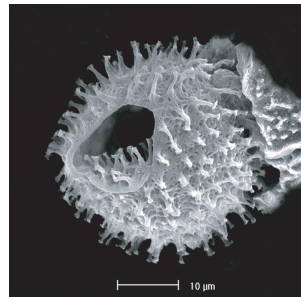
31



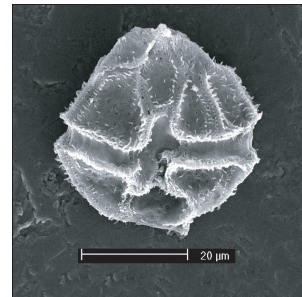
32



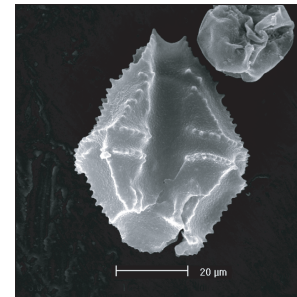
33



34

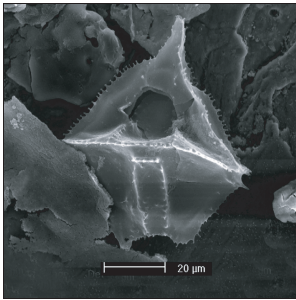


35

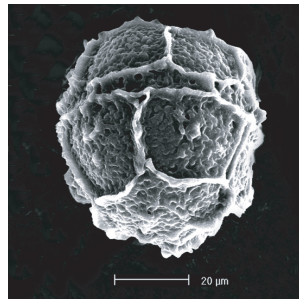


36

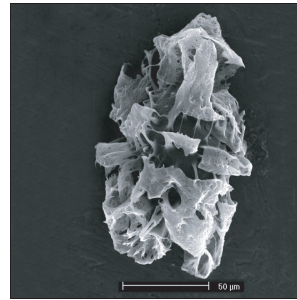
Plate P1 (continued). 37. *Spinidinium macmurdoense* (Sample 189-1172A-39X-6, 122–124 cm) (SEM). 38. *Stoveracysta kakanuiensis* (Sample 189-1172A-39X-3, 128–130 cm) (SEM). 39, 40. *Turbiosphaera filosa* (SEM); (39) Sample 189-1172A-39X-3, 48–50 cm; (40) Sample 189-1172A-39X-4, 147–149 cm. 41, 42. *Vozzhennikovia?* spp. (Sample 189-1172A-39X-3, 138–140 cm) (SEM); (41) note 3I archaeopyle; (42) note 3I operculum.



37



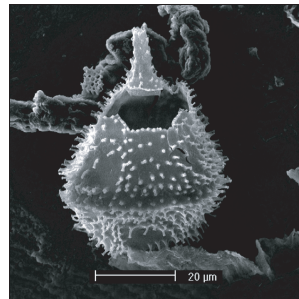
38



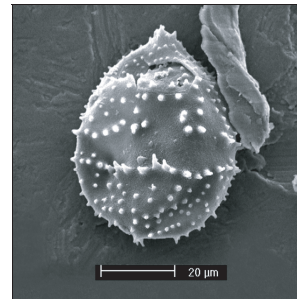
39



40



41



42

CHAPTER NOTES*

- N1. Stickley, C.E., Brinkhuis, H., Schellenberg, S.A., Sluijs, A., Fuller, M., Grauert, M., Röhl, U., Warnaar, J., and Williams, G.L., submitted. Timing and nature of the opening of the Tasmanian Gateway at the Eocene–Oligocene transition: ODP Site 1172. In Exon, N.F., Malone, M., and Kennett, J.P. (Eds.), *Cenozoic Paleocyanography and Tectonics in the Expanding Tasmanian Seaway*. Am. Geophys. Union, Geophys. Monogr.
- N2. Huber, M., Brinkhuis, H., Stickley, C.E., Döös, K., Sluijs, A., Warnaar, J., Schellenberg, S.A., and Williams, G.L., submitted. Eocene circulation of the Southern Ocean: was Antarctica kept warm by subtropical waters? *Science*.
- N3. Sluijs, A., and Brinkhuis, H., submitted. Taxonomical revision of the *Spinidinium-Vozzhennikovia* group of organic-walled, peridinooid dinoflagellate cysts. *Palaeontology*.

*Dates reflect file corrections or revisions.